Electronic Supplementary Material (ESI) for Energy & Environmental Science.

Supporting Information

Solid-State Silicon Anode with Extremely High Initial Coulombic Efficiency

Yonglin Huang,[a] Bowen Shao,[a] Yan Wang *[b] and Fudong Han *[a]

[a] Department of Mechanical, Aerospace and Nuclear Engineering, Rensselaer Polytechnic Institute, 110 8th Street, Troy, New York 12180, USA. Email: hanf2@rpi.edu
[b] Advanced Materials Lab, Samsung Advanced Institute of Technology-America, Samsung Semiconductor Inc., Cambridge, MA, USA. Email: eric.wangyan@samsung.com

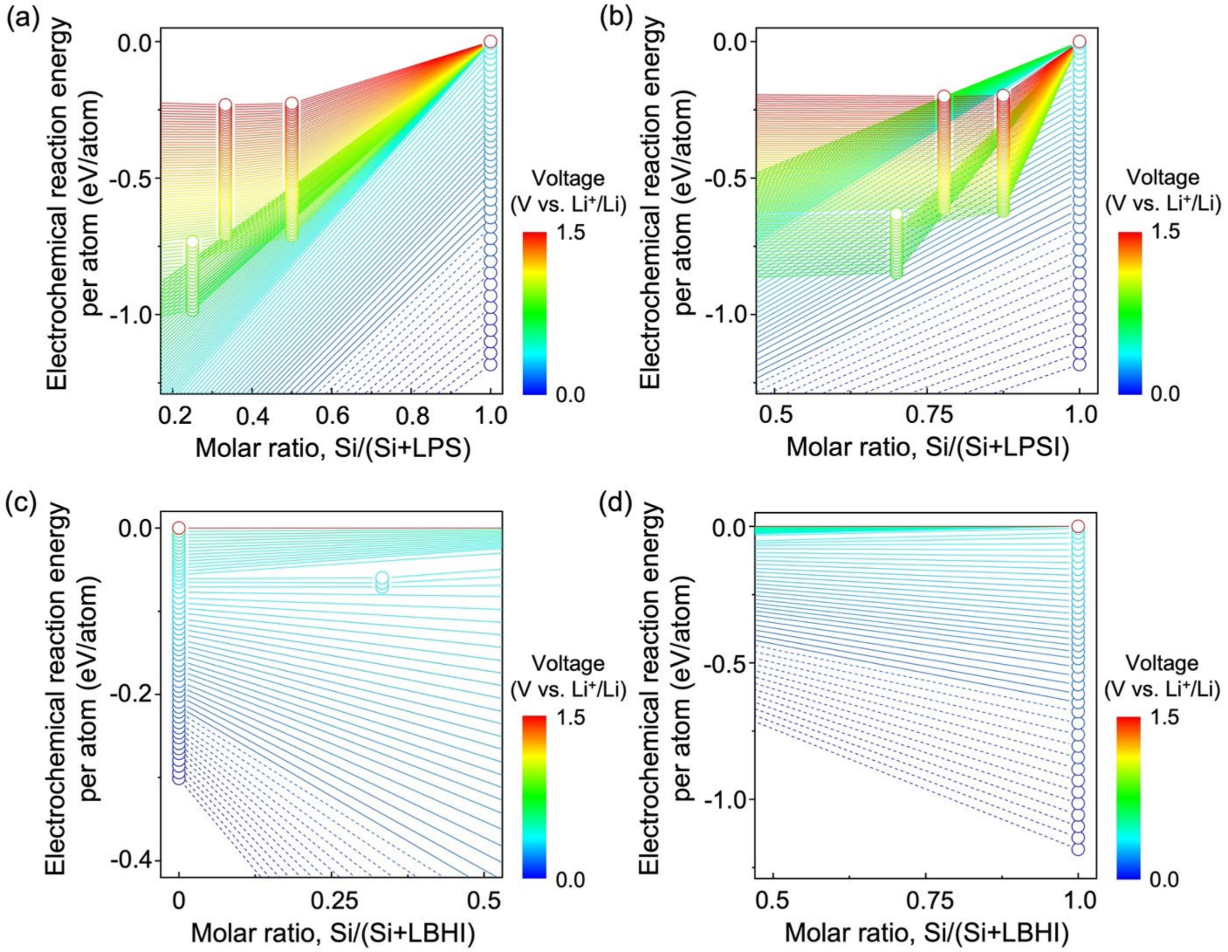

Figure S1. Magnified views of electrochemical reaction energies of Figure 1 for (a) Si-LPS, (b) Si-LPSI, and (c-d) Si-LBHI.

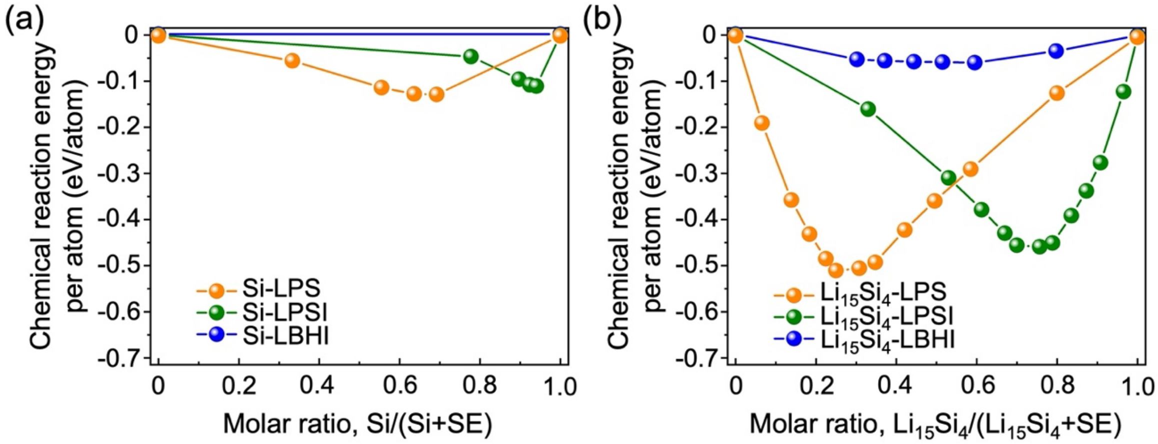

Figure S2. Calculated chemical reaction energy of (a) Si and (b) $Li_{15}Si_4$ with three SEs as a function of Si or $Li_{15}Si_4$ molar ratio.

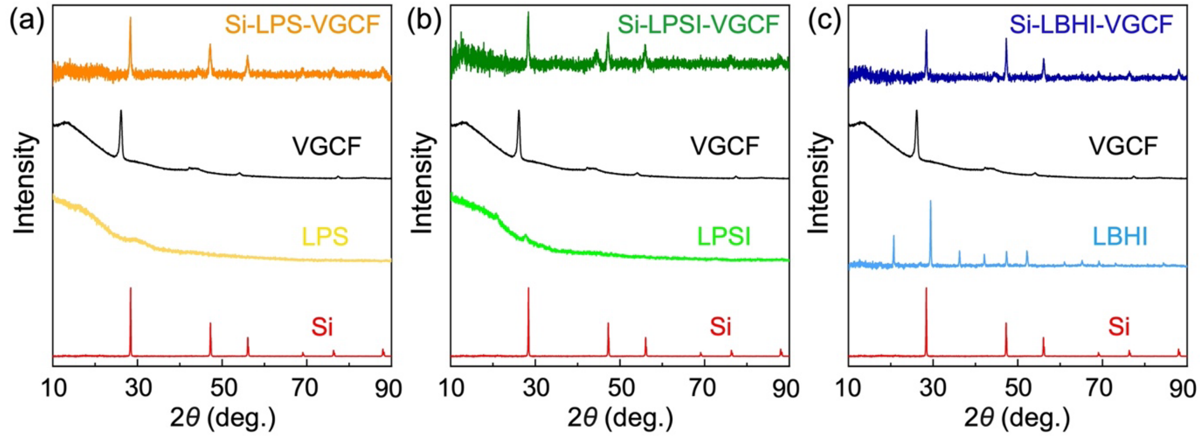

Figure S3. XRD patterns of components and ball-milled composites for (a) Si-LPS-VGCF, (b) Si-LPSI-VGCF, and (c) Si-LBHI-VGCF. The mass ratio of micro-sized Si, SE, and VGCF is 6:4:1 in the composites.

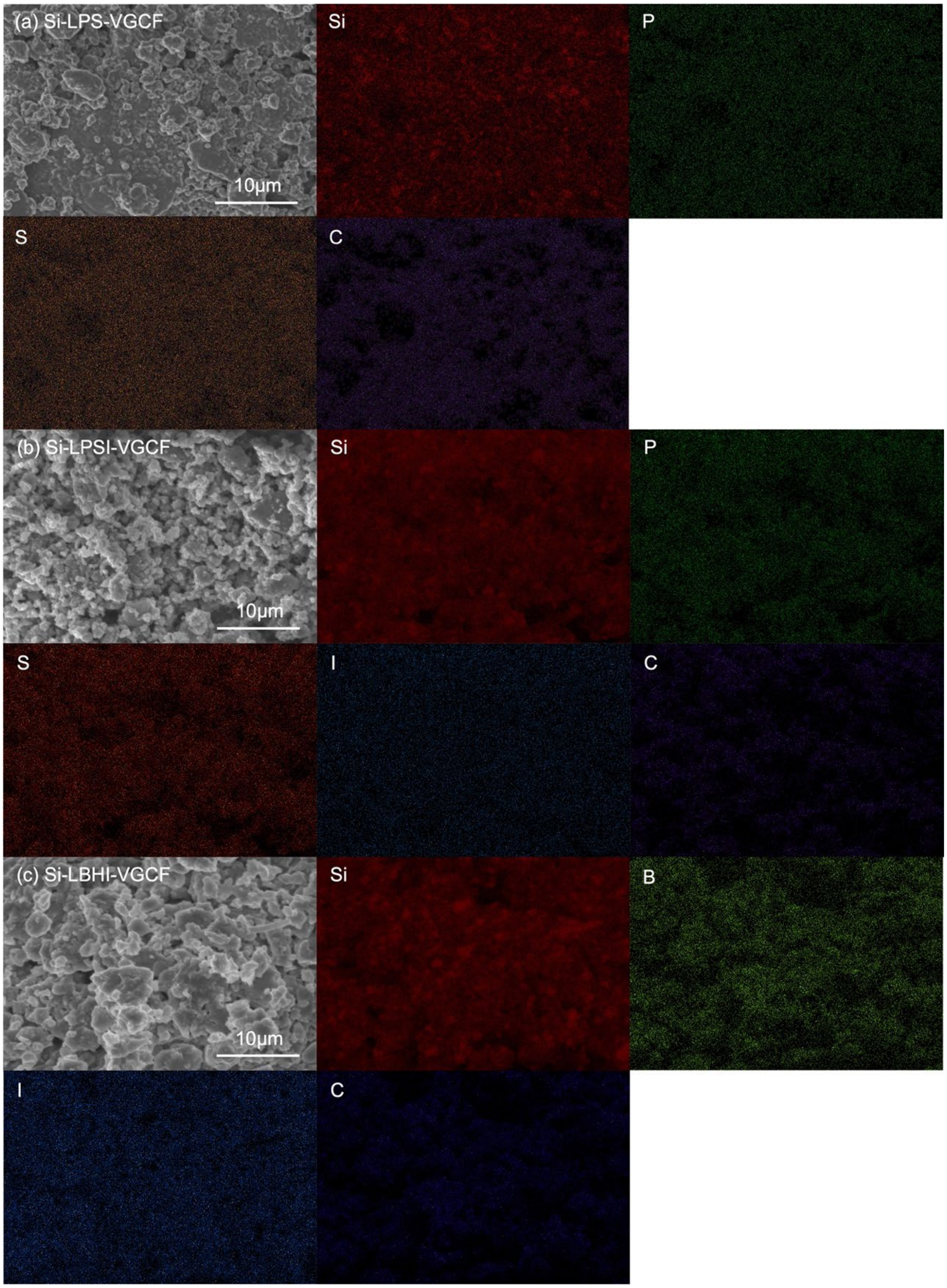

Figure S4. SEM and EDS mapping of ball-milled Si composites, (a) Si-LPS-VGCF, (b) Si-LPSI-VGCF, and (c) Si-LBHI-VGCF, with a mass ratio of 6:4:1.

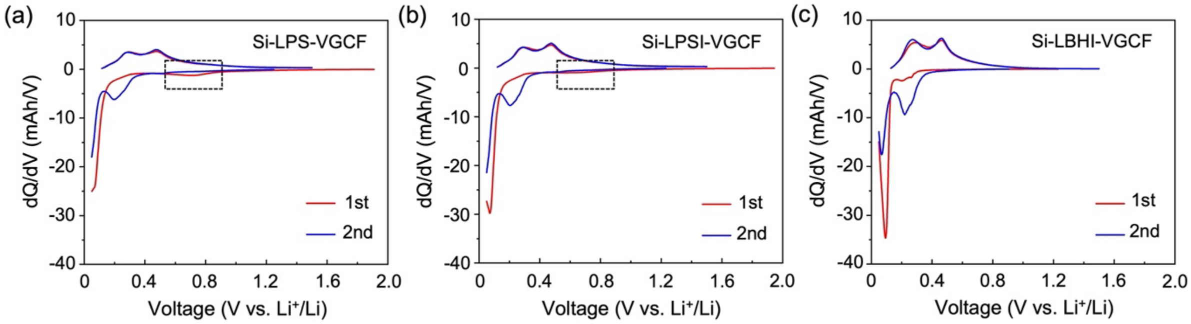

Figure S5. The differential capacity (dQ/dV) plots of (a) Si-LPS-VGCF, (b) Si-LPSI-VGCF, and (c) Si-LBHI-VGCF with a mass ratio of 6:4:1. The dashed rectangles indicate the electrochemical instability of LPS and LPSI during the first discharge.

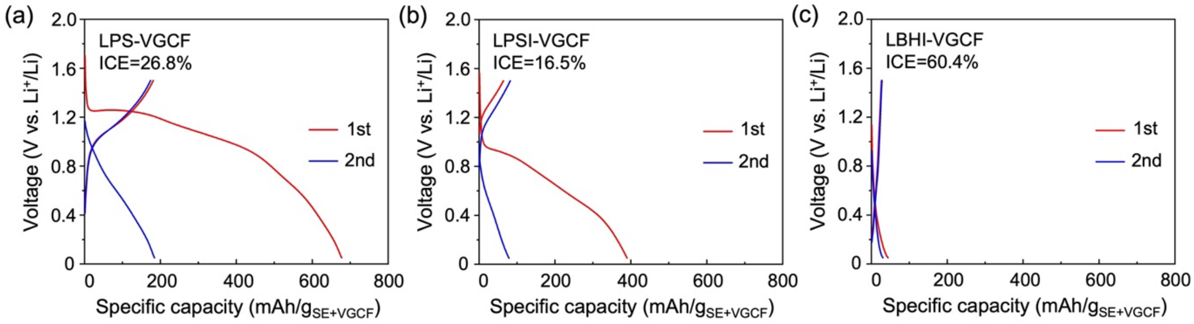

Figure S6. Voltage profiles of Li-In half cells. The anode composites, (a) LPS-VGCF, (b) LPSI-VGCF, and (c) LBHI-VGCF, were prepared by ball milling SE and VGCF in a mass ratio of 6:1. These half cells were made by the same procedure as Figure 2(a-c) with an electrode mass of 3.18 mg SE-VGCF. The current is 0.382 mA and the voltage range is 0.05 – 1.5 V vs. Li^+/Li (or -0.55 – 0.9 V vs. Li-In) at 60 °C. The small capacity in Figure S6(c) is provided by VGCF, not the decomposition of LBHI.

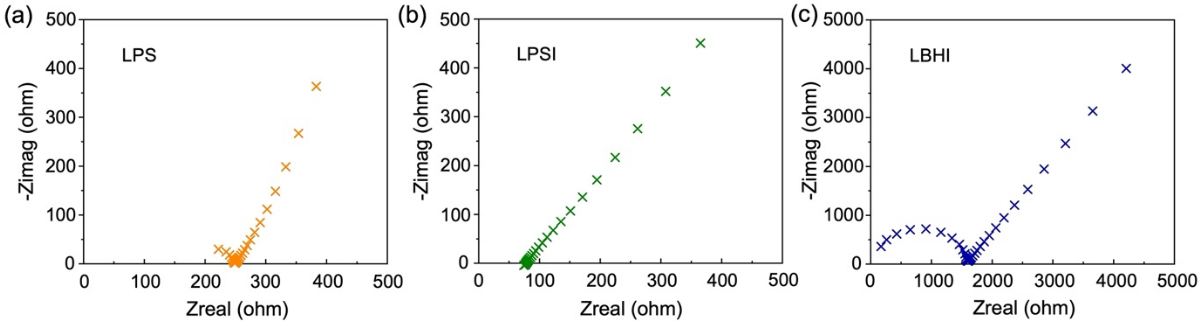

Figure S7. Nyquist plots of symmetrical cells with (a) LPS, (b) LPSI, and (c) LBHI SE at 25 °C. 200 mg SE was stacked between two stainless steel electrodes. The bulk resistance used for the calculation of ionic conductivities is obtained from the intercept of the Nyquist curve with the Zreal axis. The ionic conductivities of LPS, LPSI, and LBHI are 0.5, 1.2, and 0.1 mS/cm, respectively.

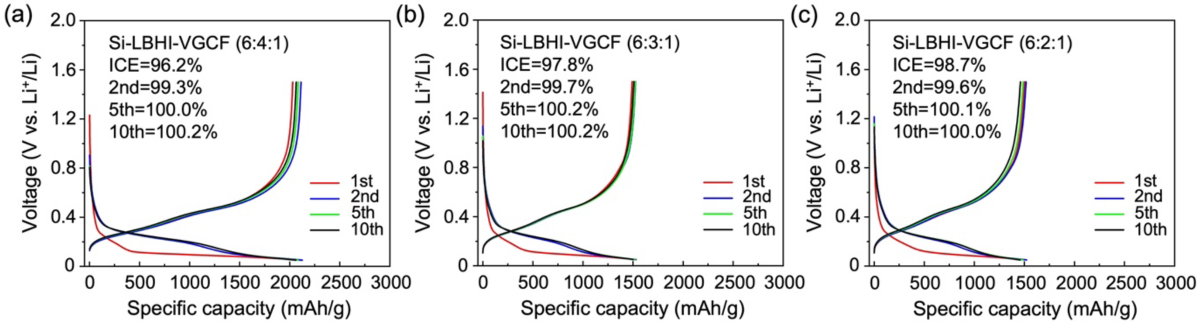

Figure S8. Charge/discharge curves of Si-LBHI-VGCF anodes with different contents of SE. The mass ratio of micro-sized Si, LBHI, and VGCF is (a) 6:4:1, (b) 6:3:1, and (c) 6:2:1, respectively. The cells are tested at a current of 210 mA/g_{Si} within the voltage range of 0.05 – 1.5 V vs. Li^+/Li (or -0.55 – 0.9 V vs. Li-In) at 60 °C.

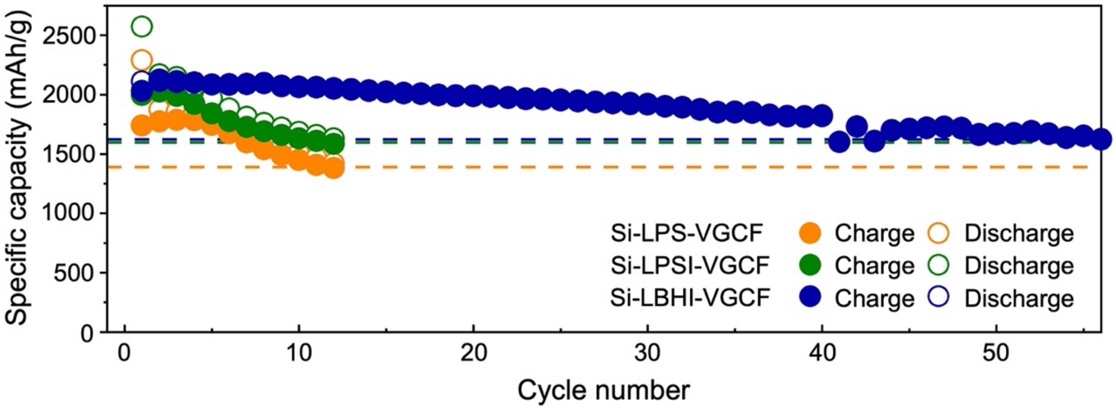

Figure S9. Long-term cycling performance of Si||Li-In half cells. The mass ratio of micro-sized Si, SE, and VGCF is 6:4:1. The dashed line indicates 80% of the first charge capacity of each half cell. The current value is 210 mA/g_{Si} and the voltage range is 0.05 – 1.5 V vs. Li^+/Li (or -0.55 – 0.9 V vs. Li-In) at 60 °C. The half cell using Si-LBHI-VGCF can stably retain 80% initial charge capacity for about 40 cycles.

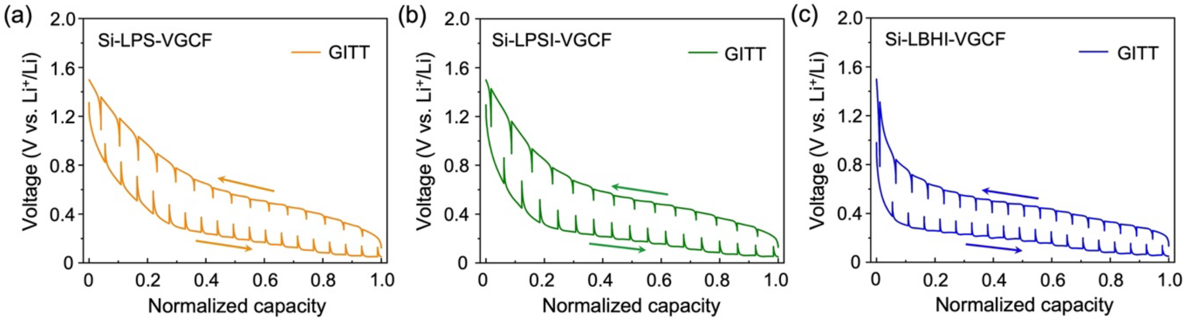

Figure S10. Voltage curves of Si||Li-In half cells during GITT tests as a function of normalized capacity. This GITT measurement (pulse time 0.5 hr, relaxation time 3 hr) was applied during the second cycle. The mass ratio of micro-sized Si, SE, and VGCF is 4:6:1 for (a) Si-LPS-VGCF, (b) Si-LPSI-VGCF, and (c) Si-LBHI-VGCF. The current value is 210 mA/g_{Si} and the voltage range is 0.05 – 1.5 V vs. Li^+/Li (or -0.55 – 0.9 V vs. Li-In) at 60 °C.

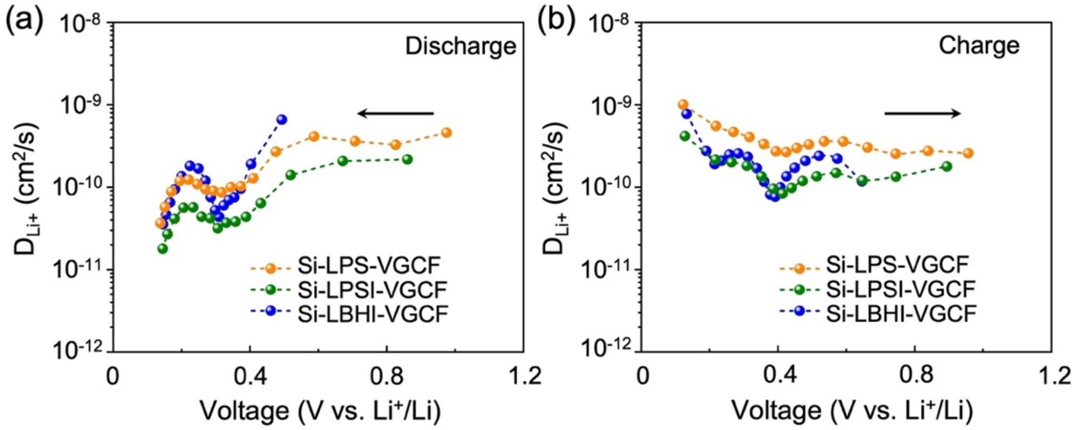

Figure S11. GITT-derived apparent lithium diffusion coefficients (D_{Li+}) for Si composites in the discharge (a) and charge (b) processes. D_{Li+} was calculated according to the below equation [1-7]:

$$D_{Li+} = \frac{4}{\pi\tau}\left(\frac{m_B V_M}{M_B S}\right)^2\left(\frac{\Delta E_s}{\Delta E_t}\right)^2 \quad (\tau << L^2/D_{Li+})$$

in which τ (= 1800 s) is the duration of the current pulse, m_B (= 0.00182 g) is the mass of active material within composites, V_M is the molar volume of Si composites, M_B (= 28.0855 g/mol) is the molar mass of Si, S (= 0.7854 cm^2) is the apparent contact area, ΔE_s is the voltage change of the steady state, and ΔE_t is the voltage change during the current pulse, neglecting the IR drop (I is the applied current, R is SE resistance).

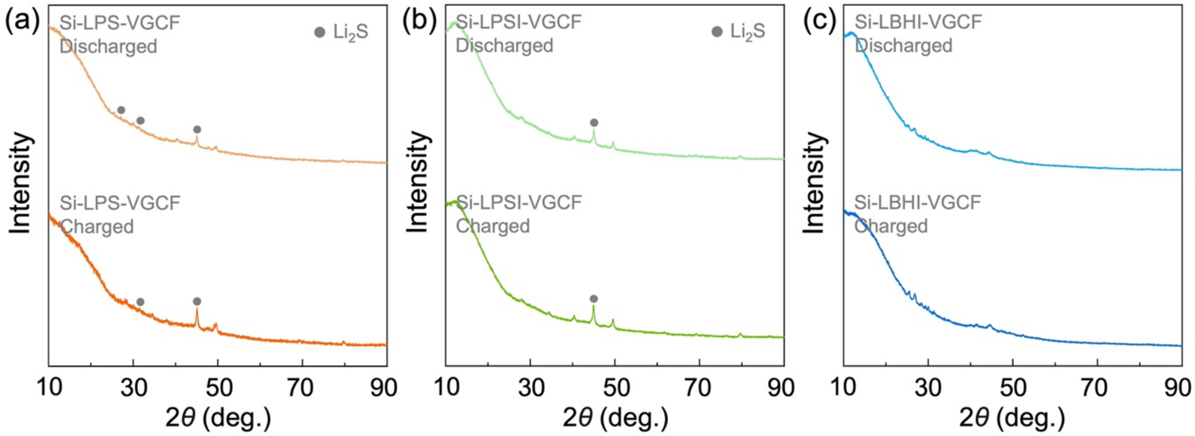

Figure S12. XRD patterns (a) Si-LPS-VGCF, (b) Si-LPSI-VGCF, and (c) Si-LBHI-VGCF after discharge (top) and after one cycle (bottom) of Si||Li-In half cells. The mass ratio of micro-sized Si, SE, and VGCF is 6:4:1 in the composites.

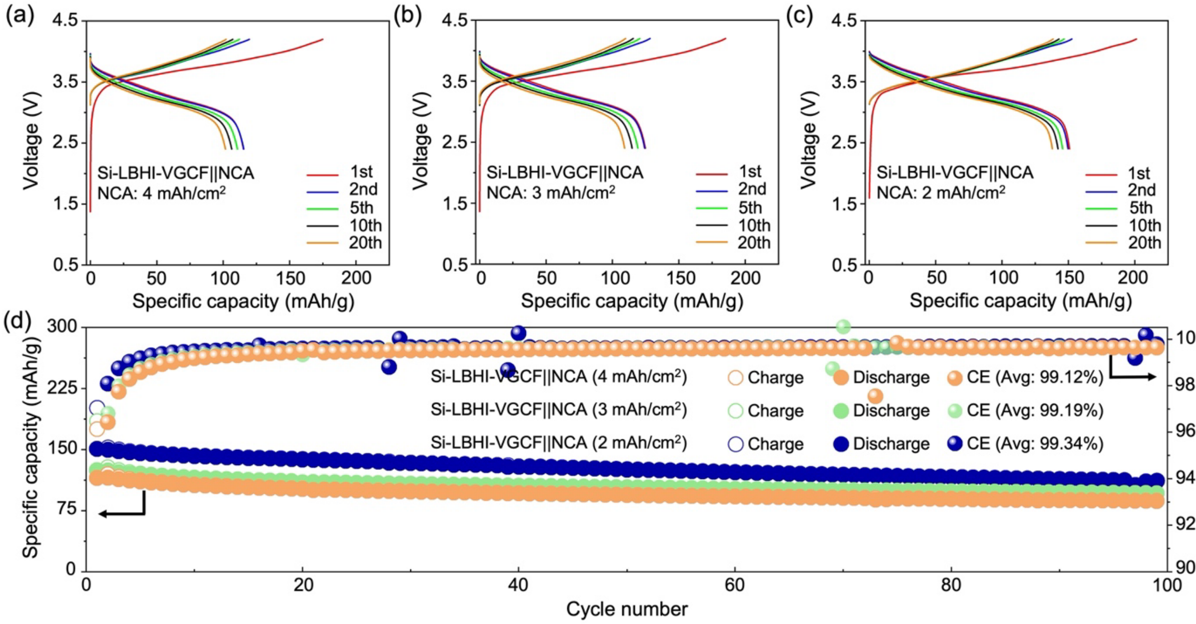

Figure S13. Charge/discharge curves of solid-state Si-LBHI-VGCF||NCA full cells with a cathode areal capacity of (a) 4.0 mAh/cm^2, (b) 3.0 mAh/cm^2, and (c) 2.0 mAh/cm^2. (d) Cycling performance and CEs of Si-LBHI-VGCF||NCA full cells with different cathode areal capacities. The NP ratio for the cells is kept at 2.74. The mass ratio of micro-sized Si, LBHI, and VGCF is 6:4:1. The cells were tested at 0.5C (based on 180 mAh/g$_{NCA}$) within a voltage range of 2.4 – 4.2 V at 60 °C.

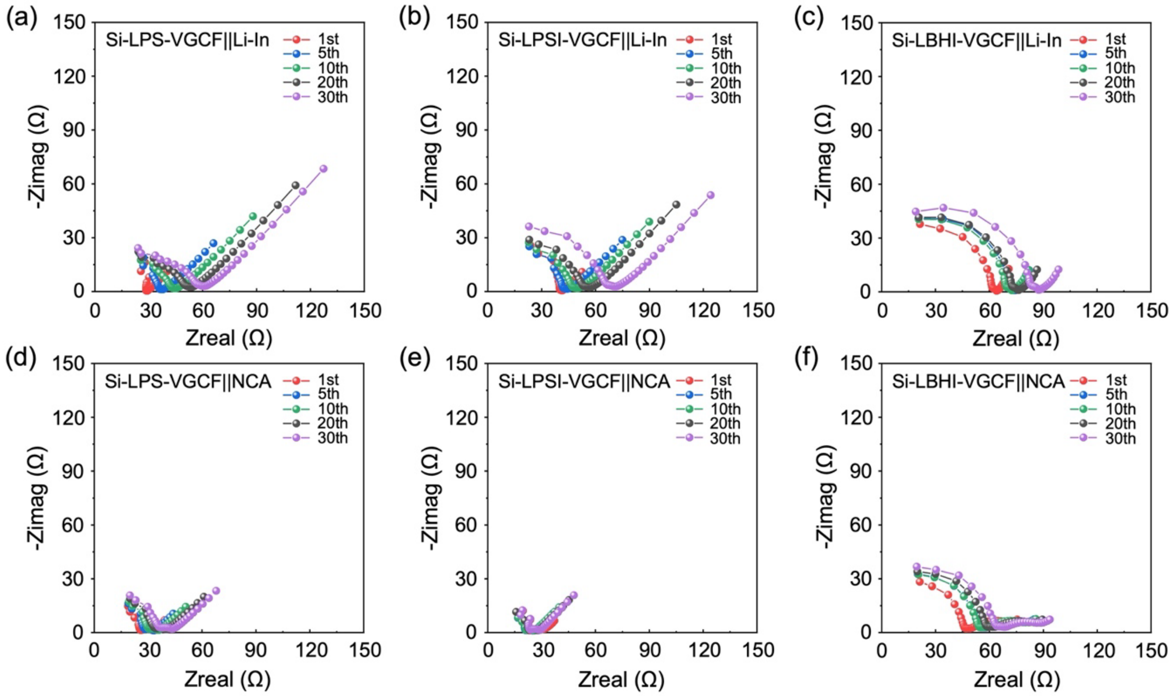

Figure S14. The Nyquist plots of (a) Si-LPS-VGCF||Li-In, (b) Si-LPSI-VGCF||Li-In, (c) Si-LBHI-VGCF||Li-In, (d) Si-LPS-VGCF||NCA, (e) Si-LPSI-VGCF||NCA, and (f) Si-LBHI-VGCF||NCA cells after different cycles. The Nyquist plots were obtained from the corresponding batteries in Figure 2(a-c) and Figure 5(a-c). The mass ratio of micro-sized Si, SE, and VGCF is 6:4:1. The PEIS data were acquired with an amplitude of 10 mV and a frequency range of 15 MHz – 1 Hz.

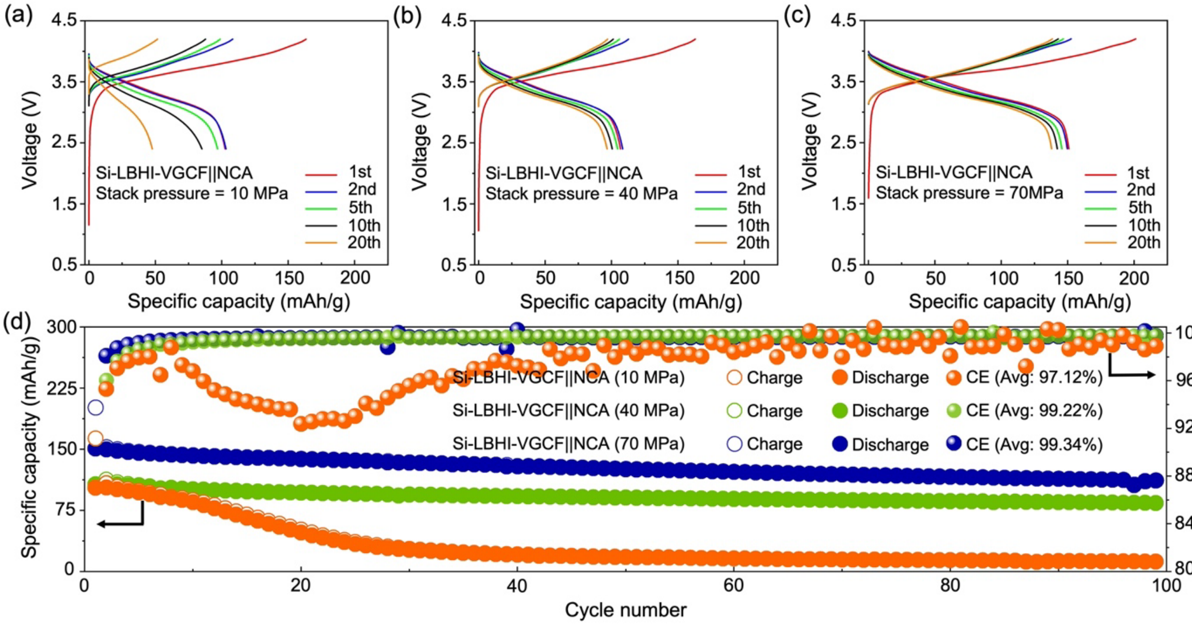

Figure S15. Charge/discharge curves of solid-state Si-LBHI-VGCF||NCA full cells under a stack pressure of (a) 10 MPa, (b) 40 MPa, and (c) 70 MPa. (d) Cycling performance and CEs of Si-LBHI-VGCF||NCA full cells under different stack pressures. The mass ratio of micro-sized Si, LBHI, and VGCF is 6:4:1. The cells were tested at 0.5C (= 0.785 mA) within a voltage range of 2.4 – 4.2 V at 60 °C. The areal capacity of the NCA cathode is 2 mAh/cm^2.

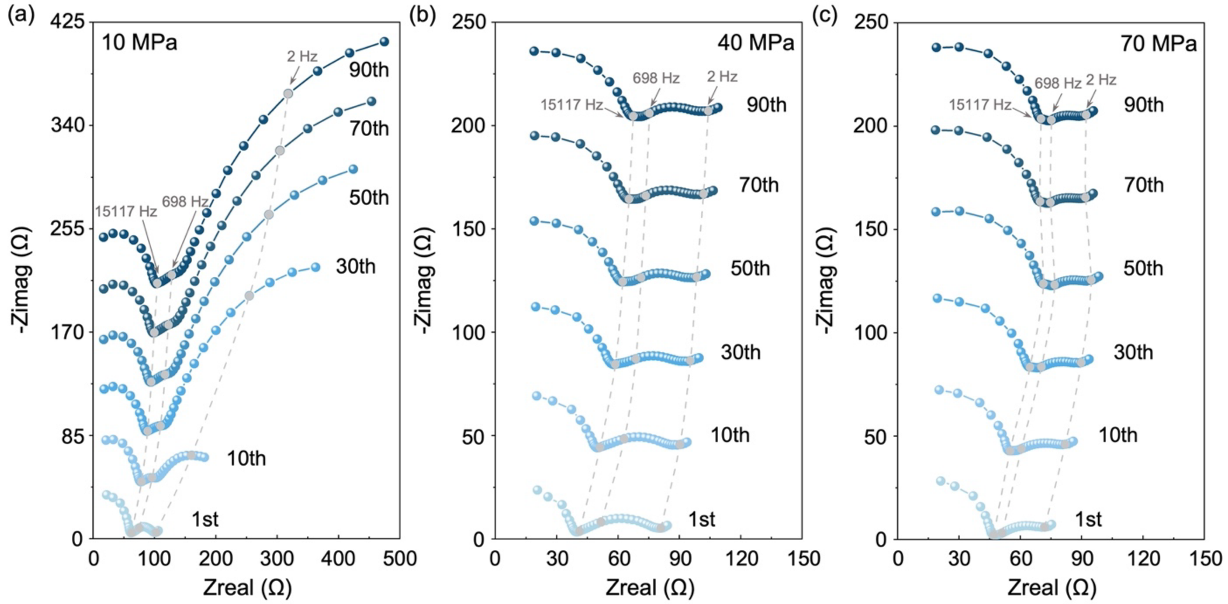

Figure S16. The evolution of impedance of Si-LBHI-VGCF||NCA full cells under different stack pressure of (a) 10 MPa, (b) 40 MPa, and (c) 70 MPa. The Nyquist plots were obtained from the corresponding batteries in Figure S15 after different cycles. The mass ratio of micro-sized Si, LBHI, and VGCF is 6:4:1. The PEIS data were acquired with an amplitude of 10 mV and a frequency range of 15 MHz – 1 Hz.

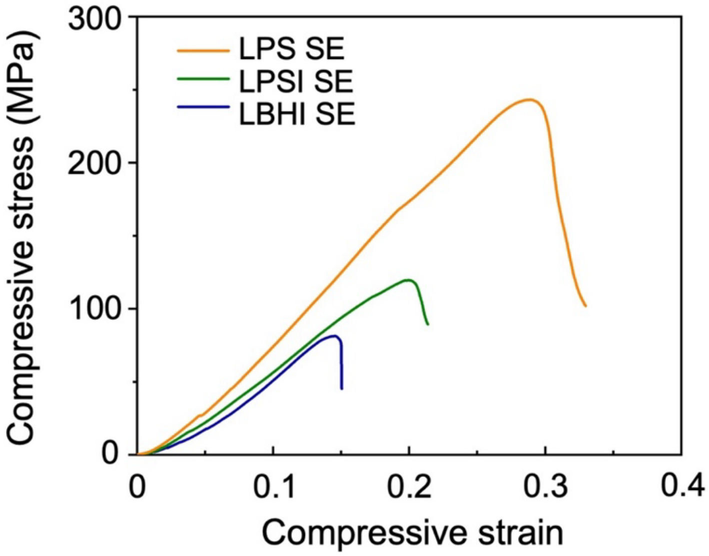

Figure S17. The compressive stress-strain curves of three cold-pressed SEs. The compression rate is 0.1 mm/min. Detailed sample parameters are shown below. All three curves show several minor pre-fracture cracks, but the stress continues to increase due to the compressive state until it reaches the peak. LBHI has a brittle fracture, as indicated by the vertical stress drop, while LPS and LPSI show ductility.

Materials	Cold-pressed cylinder		Cylinder weight/mg	Young's modulus/GPa	Peak load/N
	Diameter/mm	Height/mm			
LPS[*1]	10	1.400	197.7	1.01449	19094.42773
LPSI[*1]	10	1.195	205.4	0.76741[*2]	9389.91699
LBHI[*1]	10	1.373	162.0	0.82395[*2]	6395.18848

Note: *1. The cold-press pressure for preparing SE cylinders is 750 MPa, except LBHI. If LBHI is clod-pressed at 750 MPa, the LBHI cylinder will break when it is ejected out of the stainless-steel mold because LBHI is closely attached to the steel mold. Therefore, the maximum cold-press pressure for LBHI is 350 MPa.

*2. The modulus of LPSI is slightly smaller than that of LBHI in the above Table because the Instron system calculates the modulus of LBHI (0.82395 GPa) using the strain range of 0.1 – 0.15. Actually, the modulus of LBHI at the initial strain range of 0 – 0.05 can better reflect the intrinsic modulus, which is smaller than that of LPSI (0.76741 GPa).

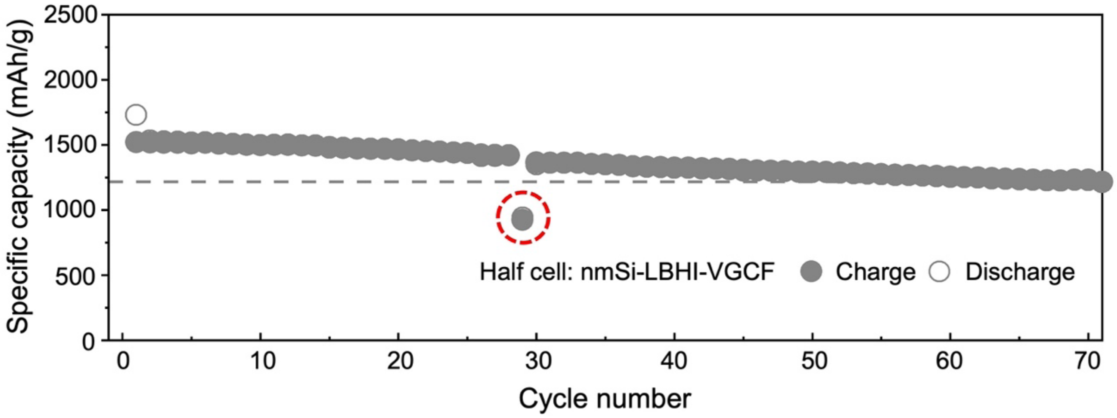

Figure S18. Long-term cycling performance of Si||Li-In half cell using nmSi composite anode. The mass ratio of nanosized Si, LBHI, and VGCF is 6:4:1. The dashed line indicates 80% of the first charge capacity. The current value is 210 mA/g_{Si} and the voltage range is 0.05 – 1.5 V vs. Li^+/Li (or -0.55 – 0.9 V vs. Li-In) at 60 °C. This half cell can retain 80% initial charge capacity for 71 cycles. The low ICE of 87.9% and low initial specific capacities should be caused by the much higher specific surface area of nanosized Si particles. Surficial silicon oxides hinder the conduction of ions and electrons. Moreover, silicon oxides lead to the irreversible consumption of lithium. And the particle size of LBHI can be further reduced to optimize the microstructure of the nmSi-LBHI-VGCF composite. The data indicated by the red circle was caused by the decreased temperature during the discharge process.

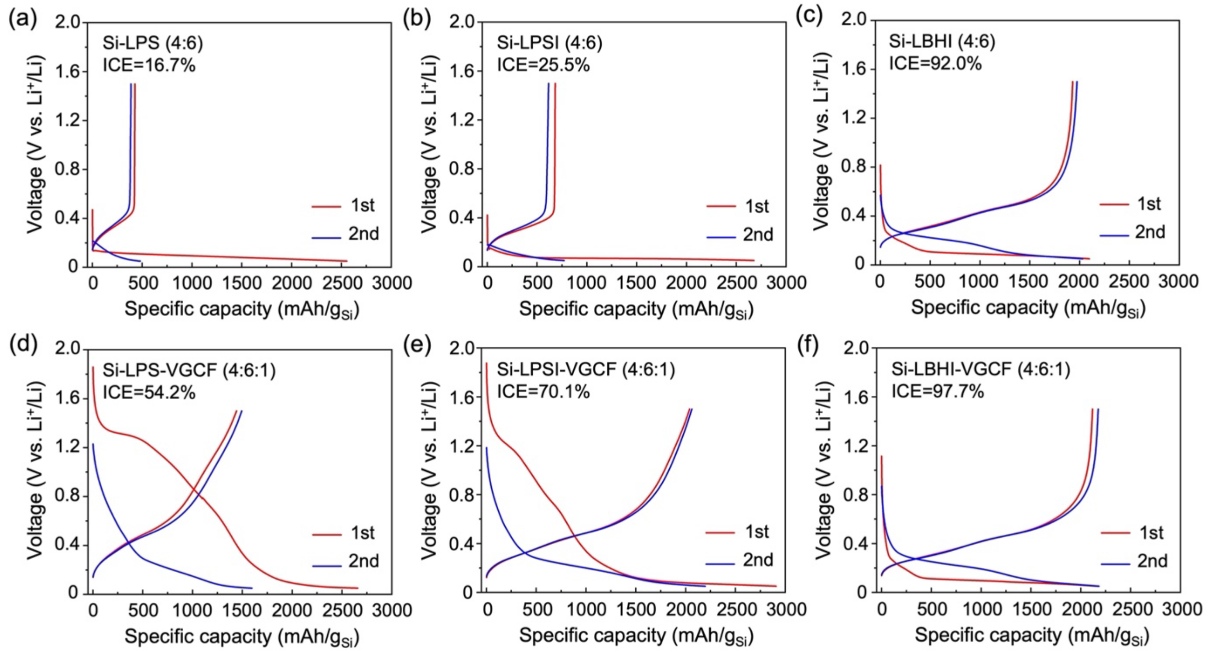

Figure S19. Voltage profiles of Si||Li-In half cells. The Si anode composites, (a) Si-LPS, (b) Si-LPSI, (c) Si-LBHI, (d) Si-LPS-VGCF, (e) Si-LPSI-VGCF, and (f) Si-LBHI-VGCF were prepared by ball milling Si and SE in a mass ratio of 4:6 for (a-c) or by ball milling Si, SE, and VGCF in a mass ratio of 4:6:1 for (d-f). These half cells were made by the same procedure as Figure 2(a-c) with an electrode mass of 4.55 mg Si-SE for (a-c) or 5 mg Si-SE-VGCF for (d-f). The current is 0.382 mA (*i.e.*, 210mA/g$_{Si}$) and the voltage range is 0.05 – 1.5 V vs. Li$^+$/Li (or -0.55 – 0.9 V vs. Li-In) at 60 °C.

References

1. A. J. Bard, L. R. Faulkner and H. S. White, *Electrochemical Methods: Fundamentals and Applications*, John Wiley & Sons, 2022.
2. H. Zhang, P. Zong, M. Chen, H. Jin, Y. Bai, S. Li, F. Ma, H. Xu and K. Lian, *ACS Nano*, 2019, **13**, 3054-3062.
3. H. Xu, Y. Wang, R. Chen, Y. Bai, T. Li, H. Jin, J. Wang and H. Xia, *Carbon*, 2020, **157**, 330-339.
4. J. H. Park, H. Yoon, Y. Cho and C.-Y. Yoo, *Materials*, 2021, **14**, 4683.
5. Y. Du, Z. Yi, Z. Zhang, J. Liao, Y. Xu, J. Bao and X. Zhou, *Chemical Engineering Journal*, 2022, **435**, 135100.
6. Y. Hu, B. Wu, H. Yi, L. Hu, R. Wang, J. Shen and B. Wang, *The Journal of Physical Chemistry C*, 2022.
7. D. Liang, Y. Lu, L. Hu, L. Wang, S. Liang, X. Liang, L. Liu, Z. Xu, C. Han and C. Liang, *Journal of Power Sources*, 2022, **544**, 231897.

Table S1. Summary of calculated electrochemical stability between Si and LPS

Voltage (V vs. Li/Li+)	Ratio, Si/LPS	Molar ratio, Si/(Si+LPS)	Reaction products	**E**rxtrxt (eV/atom)
1.49(→1.28)	0	0	P, Li2S	-0.218
	1/2	1/3=33.3%	Li2S, SiP2	-0.232
	1/1	1/2=50%	Li2S, SiP	-0.227
1.48	0	0	P, Li2S	-0.228
	1/2	1/3=33.3%	Li2S, SiP2	-0.241
	1/1	1/2=50%	Li2S, SiP	-0.235
1.47	0	0	P, Li2S	-0.238
	1/2	1/3=33.3%	Li2S, SiP2	-0.25
	1/1	1/2=50%	Li2S, SiP	-0.243
1.46	0	0	P, Li2S	-0.248
	1/2	1/3=33.3%	Li2S, SiP2	-0.259
	1/1	1/2=50%	Li2S, SiP	-0.252
1.45	0	0	P, Li2S	-0.258
	1/2	1/3=33.3%	Li2S, SiP2	-0.269
	1/1	1/2=50%	Li2S, SiP	-0.26
1.44	0	0	P, Li2S	-0.268
	1/2	1/3=33.3%	Li2S, SiP2	-0.278
	1/1	1/2=50%	Li2S, SiP	-0.268
1.43	0	0	P, Li2S	-0.278
	1/2	1/3=33.3%	Li2S, SiP2	-0.287
	1/1	1/2=50%	Li2S, SiP	-0.277
1.42	0	0	P, Li2S	-0.288
	1/2	1/3=33.3%	Li2S, SiP2	-0.296
	1/1	1/2=50%	Li2S, SiP	-0.285
1.41	0	0	P, Li2S	-0.298
	1/2	1/3=33.3%	Li2S, SiP2	-0.305
	1/1	1/2=50%	Li2S, SiP	-0.293
1.40	0	0	P, Li2S	-0.308
	1/2	1/3=33.3%	Li2S, SiP2	-0.314
	1/1	1/2=50%	Li2S, SiP	-0.302
1.39	0	0	P, Li2S	-0.318
	1/2	1/3=33.3%	Li2S, SiP2	-0.323
	1/1	1/2=50%	Li2S, SiP	-0.31
1.38	0	0	P, Li2S	-0.328
	1/2	1/3=33.3%	Li2S, SiP2	-0.332
	1/1	1/2=50%	Li2S, SiP	-0.318
1.37	0	0	P, Li2S	-0.338
	1/2	1/3=33.3%	Li2S, SiP2	-0.341
	1/1	1/2=50%	Li2S, SiP	-0.327

1.36	0	0	P, Li2S	-0.348
	1/2	1/3=33.3%	Li2S, SiP2	-0.35
	1/1	1/2=50%	Li2S, SiP	-0.335
1.35	0	0	P, Li2S	-0.358
	1/2	1/3=33.3%	Li2S, SiP2	-0.359
	1/1	1/2=50%	Li2S, SiP	-0.343
1.34	0	0	P, Li2S	-0.368
	1/2	1/3=33.3%	Li2S, SiP2	-0.369
	1/1	1/2=50%	Li2S, SiP	-0.352
1.33	0	0	P, Li2S	-0.378
	1/2	1/3=33.3%	Li2S, SiP2	-0.378
	1/1	1/2=50%	Li2S, SiP	-0.36
1.32	0	0	P, Li2S	-0.388
	1/2	1/3=33.3%	Li2S, SiP2	-0.387
	1/1	1/2=50%	Li2S, SiP	-0.368
1.31	0	0	P, Li2S	-0.398
	1/2	1/3=33.3%	Li2S, SiP2	-0.396
	1/1	1/2=50%	Li2S, SiP	-0.377
1.30	0	0	P, Li2S	-0.408
	1/2	1/3=33.3%	Li2S, SiP2	-0.405
	1/1	1/2=50%	Li2S, SiP	-0.385
1.29	0	0	P, Li2S	-0.418
	1/2	1/3=33.3%	Li2S, SiP2	-0.414
	1/1	1/2=50%	Li2S, SiP	-0.393
1.28	0	0	P, Li2S	-0.428
	1/2	1/3=33.3%	Li2S, SiP2	-0.423
	1/1	1/2=50%	Li2S, SiP	-0.402
1.27(→1.17)	0	0	LiP7, Li2S	-0.438
	1/2	1/3=33.3%	Li2S, SiP2	-0.432
	1/1	1/2=50%	Li2S, SiP	-0.41
1.26	0	0	LiP7, Li2S	-0.448
	1/2	1/3=33.3%	Li2S, SiP2	-0.441
	1/1	1/2=50%	Li2S, SiP	-0.418
1.25	0	0	LiP7, Li2S	-0.458
	1/2	1/3=33.3%	Li2S, SiP2	-0.45
	1/1	1/2=50%	Li2S, SiP	-0.427
1.24	0	0	LiP7, Li2S	-0.469
	1/2	1/3=33.3%	Li2S, SiP2	-0.459
	1/1	1/2=50%	Li2S, SiP	-0.435
1.23	0	0	LiP7, Li2S	-0.479
	1/2	1/3=33.3%	Li2S, SiP2	-0.469
	1/1	1/2=50%	Li2S, SiP	-0.443

1.22	0	0	LiP7, Li2S	-0.489
	1/2	1/3=33.3%	Li2S, SiP2	-0.478
	1/1	1/2=50%	Li2S, SiP	-0.452
1.21	0	0	LiP7, Li2S	-0.499
	1/2	1/3=33.3%	Li2S, SiP2	-0.487
	1/1	1/2=50%	Li2S, SiP	-0.46
1.20	0	0	LiP7, Li2S	-0.51
	1/2	1/3=33.3%	Li2S, SiP2	-0.496
	1/1	1/2=50%	Li2S, SiP	-0.468
1.19	0	0	LiP7, Li2S	-0.52
	1/2	1/3=33.3%	Li2S, SiP2	-0.505
	1/1	1/2=50%	Li2S, SiP	-0.477
1.18	0	0	LiP7, Li2S	-0.53
	1/2	1/3=33.3%	Li2S, SiP2	-0.514
	1/1	1/2=50%	Li2S, SiP	-0.485
1.17	0	0	LiP7, Li2S	-0.541
	1/2	1/3=33.3%	Li2S, SiP2	-0.523
	1/1	1/2=50%	Li2S, SiP	-0.493
1.16(→0.97)	0	0	Li3P7, Li2S	-0.551
	1/2	1/3=33.3%	Li2S, SiP2	-0.532
	1/1	1/2=50%	Li2S, SiP	-0.502
1.15	0	0	Li3P7, Li2S	-0.562
	1/2	1/3=33.3%	Li2S, SiP2	-0.541
	1/1	1/2=50%	Li2S, SiP	-0.51
1.14	0	0	Li3P7, Li2S	-0.573
	1/2	1/3=33.3%	Li2S, SiP2	-0.55
	1/1	1/2=50%	Li2S, SiP	-0.518
1.13	0	0	Li3P7, Li2S	-0.584
	1/2	1/3=33.3%	Li2S, SiP2	-0.559
	1/1	1/2=50%	Li2S, SiP	-0.527
1.12	0	0	Li3P7, Li2S	-0.594
	1/2	1/3=33.3%	Li2S, SiP2	-0.569
	1/1	1/2=50%	Li2S, SiP	-0.535
1.11	0	0	Li3P7, Li2S	-0.605
	1/2	1/3=33.3%	Li2S, SiP2	-0.578
	1/1	1/2=50%	Li2S, SiP	-0.543
1.10	0	0	Li3P7, Li2S	-0.616
	1/2	1/3=33.3%	Li2S, SiP2	-0.587
	1/1	1/2=50%	Li2S, SiP	-0.552
1.09	0	0	Li3P7, Li2S	-0.627
	1/2	1/3=33.3%	Li2S, SiP2	-0.596
	1/1	1/2=50%	Li2S, SiP	-0.56

1.08	0	0	Li3P7, Li2S	-0.638
	1/2	1/3=33.3%	Li2S, SiP2	-0.605
	1/1	1/2=50%	Li2S, SiP	-0.568
1.07	0	0	Li3P7, Li2S	-0.649
	1/2	1/3=33.3%	Li2S, SiP2	-0.614
	1/1	1/2=50%	Li2S, SiP	-0.577
1.06	0	0	Li3P7, Li2S	-0.66
	1/2	1/3=33.3%	Li2S, SiP2	-0.623
	1/1	1/2=50%	Li2S, SiP	-0.585
1.05	0	0	Li3P7, Li2S	-0.67
	1/2	1/3=33.3%	Li2S, SiP2	-0.632
	1/1	1/2=50%	Li2S, SiP	-0.593
1.04	0	0	Li3P7, Li2S	-0.681
	1/2	1/3=33.3%	Li2S, SiP2	-0.641
	1/1	1/2=50%	Li2S, SiP	-0.602
1.03	0	0	Li3P7, Li2S	-0.692
	1/2	1/3=33.3%	Li2S, SiP2	-0.65
	1/1	1/2=50%	Li2S, SiP	-0.61
1.02	0	0	Li3P7, Li2S	-0.703
	1/2	1/3=33.3%	Li2S, SiP2	-0.659
	1/1	1/2=50%	Li2S, SiP	-0.618
1.01	0	0	Li3P7, Li2S	-0.714
	1/2	1/3=33.3%	Li2S, SiP2	-0.669
	1/1	1/2=50%	Li2S, SiP	-0.627
1.00	0	0	Li3P7, Li2S	-0.725
	1/2	1/3=33.3%	Li2S, SiP2	-0.678
	1/1	1/2=50%	Li2S, SiP	-0.635
0.99	0	0	Li3P7, Li2S	-0.736
	1/2	1/3=33.3%	Li2S, SiP2	-0.687
	1/1	1/2=50%	Li2S, SiP	-0.643
0.98	0	0	Li3P7, Li2S	-0.746
	1/2	1/3=33.3%	Li2S, SiP2	-0.696
	1/1	1/2=50%	Li2S, SiP	-0.652
0.97	0	0	Li3P7, Li2S	-0.757
	1/2	1/3=33.3%	Li2S, SiP2	-0.705
	1/1	1/2=50%	Li2S, SiP	-0.66
0.96(→0.94)	0	0	Li3P7, Li2S	-0.768
	1/3	1/4=25%	Li2S, Li5SiP3	-0.733
	1/1	1/2=50%	Li2S, SiP	-0.668
0.95	0	0	Li3P7, Li2S	-0.779
	1/3	1/4=25%	Li2S, Li5SiP3	-0.746
	1/1	1/2=50%	Li2S, SiP	-0.677

0.94	0	0	Li3P7, Li2S	-0.79
	1/3	1/4=25%	Li2S, Li5SiP3	-0.758
	1/1	1/2=50%	Li2S, SiP	-0.685
0.93(→0.91)	0	0	LiP, Li2S	-0.801
	1/3	1/4=25%	Li2S, Li5SiP3	-0.771
	1/1	1/2=50%	Li2S, SiP	-0.693
0.92	0	0	LiP, Li2S	-0.813
	1/3	1/4=25%	Li2S, Li5SiP3	-0.783
	1/1	1/2=50%	Li2S, SiP	-0.702
0.91	0	0	LiP, Li2S	-0.825
	1/3	1/4=25%	Li2S, Li5SiP3	-0.796
	1/1	1/2=50%	Li2S, SiP	-0.71
0.90(→0.87)	0	0	LiP, Li2S	-0.837
	1/3	1/4=25%	Li2S, Li5SiP3	-0.808
0.89	0	0	LiP, Li2S	-0.849
	1/3	1/4=25%	Li2S, Li5SiP3	-0.821
0.88	0	0	LiP, Li2S	-0.861
	1/3	1/4=25%	Li2S, Li5SiP3	-0.833
0.87	0	0	LiP, Li2S	-0.873
	1/3	1/4=25%	Li2S, Li5SiP3	-0.846
0.86(→0.76)	0	0	Li3P, Li2S	-0.889
	1/3	1/4=25%	Li2S, Li5SiP3	-0.858
0.85	0	0	Li3P, Li2S	-0.905
	1/3	1/4=25%	Li2S, Li5SiP3	-0.871
0.84	0	0	Li3P, Li2S	-0.921
	1/3	1/4=25%	Li2S, Li5SiP3	-0.883
0.83	0	0	Li3P, Li2S	-0.937
	1/3	1/4=25%	Li2S, Li5SiP3	-0.896
0.82	0	0	Li3P, Li2S	-0.953
	1/3	1/4=25%	Li2S, Li5SiP3	-0.908
0.81	0	0	Li3P, Li2S	-0.969
	1/3	1/4=25%	Li2S, Li5SiP3	-0.921
0.80	0	0	Li3P, Li2S	-0.985
	1/3	1/4=25%	Li2S, Li5SiP3	-0.933
0.79	0	0	Li3P, Li2S	-1.001
	1/3	1/4=25%	Li2S, Li5SiP3	-0.946
0.78	0	0	Li3P, Li2S	-1.017
	1/3	1/4=25%	Li2S, Li5SiP3	-0.958
0.77	0	0	Li3P, Li2S	-1.033
	1/3	1/4=25%	Li2S, Li5SiP3	-0.971
0.76	0	0	Li3P, Li2S	-1.049
	1/3	1/4=25%	Li2S, Li5SiP3	-0.983

0.75(→0.40)	0	0	Li3P, Li2S	-1.065
0.74	0	0	Li3P, Li2S	-1.081
0.73	0	0	Li3P, Li2S	-1.097
0.72	0	0	Li3P, Li2S	-1.113
0.71	0	0	Li3P, Li2S	-1.129
0.7	0	0	Li3P, Li2S	-1.145
0.69	0	0	Li3P, Li2S	-1.161
0.68	0	0	Li3P, Li2S	-1.177
0.67	0	0	Li3P, Li2S	-1.193
0.66	0	0	Li3P, Li2S	-1.209
0.65	0	0	Li3P, Li2S	-1.225
0.64	0	0	Li3P, Li2S	-1.241
0.63	0	0	Li3P, Li2S	-1.257
0.62	0	0	Li3P, Li2S	-1.273
0.61	0	0	Li3P, Li2S	-1.289
0.6	0	0	Li3P, Li2S	-1.305
0.59	0	0	Li3P, Li2S	-1.321
0.58	0	0	Li3P, Li2S	-1.337
0.57	0	0	Li3P, Li2S	-1.353
0.56	0	0	Li3P, Li2S	-1.369
0.55	0	0	Li3P, Li2S	-1.385
0.54	0	0	Li3P, Li2S	-1.401
0.53	0	0	Li3P, Li2S	-1.417
0.52	0	0	Li3P, Li2S	-1.433
0.51	0	0	Li3P, Li2S	-1.449
0.5	0	0	Li3P, Li2S	-1.465
0.49	0	0	Li3P, Li2S	-1.481
0.48	0	0	Li3P, Li2S	-1.497
0.47	0	0	Li3P, Li2S	-1.513
0.46	0	0	Li3P, Li2S	-1.529
0.45	0	0	Li3P, Li2S	-1.545
0.44	0	0	Li3P, Li2S	-1.561
0.43	0	0	Li3P, Li2S	-1.577
0.42	0	0	Li3P, Li2S	-1.593
0.41	0	0	Li3P, Li2S	-1.609
0.4	0	0	Li3P, Li2S	-1.625
0.39	0	0	Li3P, Li2S	-1.641
		1	LiSi	-0.007
0.38(→0.37)	0	0	Li3P, Li2S	-1.657
		1	Li12Si7	-0.024
0.37	0	0	Li3P, Li2S	-1.673
		1	Li12Si7	-0.041

0.36(→0.18)	0	0	Li3P, Li2S	-1.689
		1	Li7Si3	-0.064
0.35	0	0	Li3P, Li2S	-1.705
		1	Li7Si3	-0.087
0.34	0	0	Li3P, Li2S	-1.721
		1	Li7Si3	-0.11
0.33	0	0	Li3P, Li2S	-1.737
		1	Li7Si3	-0.134
0.32	0	0	Li3P, Li2S	-1.753
		1	Li7Si3	-0.157
0.31	0	0	Li3P, Li2S	-1.769
		1	Li7Si3	-0.18
0.3	0	0	Li3P, Li2S	-1.785
		1	Li7Si3	-0.204
0.29	0	0	Li3P, Li2S	-1.801
		1	Li7Si3	-0.227
0.28	0	0	Li3P, Li2S	-1.817
		1	Li7Si3	-0.25
0.27	0	0	Li3P, Li2S	-1.833
		1	Li7Si3	-0.274
0.26	0	0	Li3P, Li2S	-1.849
		1	Li7Si3	-0.297
0.25	0	0	Li3P, Li2S	-1.865
		1	Li7Si3	-0.32
0.24	0	0	Li3P, Li2S	-1.881
		1	Li7Si3	-0.344
0.23	0	0	Li3P, Li2S	-1.897
		1	Li7Si3	-0.367
0.22	0	0	Li3P, Li2S	-1.913
		1	Li7Si3	-0.39
0.21	0	0	Li3P, Li2S	-1.929
		1	Li7Si3	-0.414
0.2	0	0	Li3P, Li2S	-1.945
		1	Li7Si3	-0.437
0.19	0	0	Li3P, Li2S	-1.961
		1	Li7Si3	-0.46
0.18	0	0	Li3P, Li2S	-1.977
		1	Li7Si3	-0.484
0.17(→0.13)	0	0	Li3P, Li2S	-1.993
		1	Li13Si4	-0.515
0.16	0	0	Li3P, Li2S	-2.009
		1	Li13Si4	-0.548

0.15	0	0	Li3P, Li2S	-2.025
		1	Li13Si4	-0.58
0.14	0	0	Li3P, Li2S	-2.041
		1	Li13Si4	-0.613
0.13	0	0	Li3P, Li2S	-2.057
		1	Li13Si4	-0.645
0.12(→0)	0	0	Li3P, Li2S	-2.073
		1	Li21Si5 (dashed)	-0.679
0.11	0	0	Li3P, Li2S	-2.089
		1	Li21Si5 (dashed)	-0.721
0.1	0	0	Li3P, Li2S	-2.105
		1	Li21Si5 (dashed)	-0.763
0.09	0	0	Li3P, Li2S	-2.121
		1	Li21Si5 (dashed)	-0.805
0.08	0	0	Li3P, Li2S	-2.137
		1	Li21Si5 (dashed)	-0.847
0.07	0	0	Li3P, Li2S	-2.153
		1	Li21Si5 (dashed)	-0.889
0.06	0	0	Li3P, Li2S	-2.169
		1	Li21Si5 (dashed)	-0.931
0.05	0	0	Li3P, Li2S	-2.185
		1	Li21Si5 (dashed)	-0.973
0.04	0	0	Li3P, Li2S	-2.201
		1	Li21Si5 (dashed)	-1.015
0.03	0	0	Li3P, Li2S	-2.217
		1	Li21Si5 (dashed)	-1.057
0.02	0	0	Li3P, Li2S	-2.233
		1	Li21Si5 (dashed)	-1.099
0.01	0	0	Li3P, Li2S	-2.249
		1	Li21Si5 (dashed)	-1.141
0	0	0	Li3P, Li2S	-2.265
		1	Li21Si5 (dashed)	-1.183

Table S2. Summary of calculated electrochemical stability between Si and LPSI

Voltage (V vs. Li/Li+)	Ratio, Si/LPSI	Molar ratio, Si/(Si+LPSI)	Reaction products	**E**rxtrxt (eV/atom)
1.49(→1.28)	0	0	P, Li2S, LiI	-0.186
	7/2	7/9=77.8%	Li2S, SiP2, LiI	-0.201
	7/1	7/8=87.5%	Li2S, SiP, LiI	-0.198
1.48	0	0	P, Li2S, LiI	-0.194
	7/2	7/9=77.8%	Li2S, SiP2, LiI	-0.209
	7/1	7/8=87.5%	Li2S, SiP, LiI	-0.206
1.47	0	0	P, Li2S, LiI	-0.203
	7/2	7/9=77.8%	Li2S, SiP2, LiI	-0.217
	7/1	7/8=87.5%	Li2S, SiP, LiI	-0.213
1.46	0	0	P, Li2S, LiI	-0.211
	7/2	7/9=77.8%	Li2S, SiP2, LiI	-0.224
	7/1	7/8=87.5%	Li2S, SiP, LiI	-0.22
1.45	0	0	P, Li2S, LiI	-0.22
	7/2	7/9=77.8%	Li2S, SiP2, LiI	-0.232
	7/1	7/8=87.5%	Li2S, SiP, LiI	-0.228
1.44	0	0	P, Li2S, LiI	-0.228
	7/2	7/9=77.8%	Li2S, SiP2, LiI	-0.24
	7/1	7/8=87.5%	Li2S, SiP, LiI	-0.235
1.43	0	0	P, Li2S, LiI	-0.237
	7/2	7/9=77.8%	Li2S, SiP2, LiI	-0.248
	7/1	7/8=87.5%	Li2S, SiP, LiI	-0.242
1.42	0	0	P, Li2S, LiI	-0.246
	7/2	7/9=77.8%	Li2S, SiP2, LiI	-0.256
	7/1	7/8=87.5%	Li2S, SiP, LiI	-0.249
1.41	0	0	P, Li2S, LiI	-0.254
	7/2	7/9=77.8%	Li2S, SiP2, LiI	-0.264
	7/1	7/8=87.5%	Li2S, SiP, LiI	-0.257
1.40	0	0	P, Li2S, LiI	-0.263
	7/2	7/9=77.8%	Li2S, SiP2, LiI	-0.272
	7/1	7/8=87.5%	Li2S, SiP, LiI	-0.264
1.39	0	0	P, Li2S, LiI	-0.271
	7/2	7/9=77.8%	Li2S, SiP2, LiI	-0.28
	7/1	7/8=87.5%	Li2S, SiP, LiI	-0.271
1.38	0	0	P, Li2S, LiI	-0.28
	7/2	7/9=77.8%	Li2S, SiP2, LiI	-0.287
	7/1	7/8=87.5%	Li2S, SiP, LiI	-0.279
1.37	0	0	P, Li2S, LiI	-0.288
	7/2	7/9=77.8%	Li2S, SiP2, LiI	-0.295
	7/1	7/8=87.5%	Li2S, SiP, LiI	-0.286

1.36	0	0	P, Li2S, LiI	-0.297
	7/2	7/9=77.8%	Li2S, SiP2, LiI	-0.303
	7/1	7/8=87.5%	Li2S, SiP, LiI	-0.293
1.35	0	0	P, Li2S, LiI	-0.305
	7/2	7/9=77.8%	Li2S, SiP2, LiI	-0.311
	7/1	7/8=87.5%	Li2S, SiP, LiI	-0.301
1.34	0	0	P, Li2S, LiI	-0.314
	7/2	7/9=77.8%	Li2S, SiP2, LiI	-0.319
	7/1	7/8=87.5%	Li2S, SiP, LiI	-0.308
1.33	0	0	P, Li2S, LiI	-0.322
	7/2	7/9=77.8%	Li2S, SiP2, LiI	-0.327
	7/1	7/8=87.5%	Li2S, SiP, LiI	-0.315
1.32	0	0	P, Li2S, LiI	-0.331
	7/2	7/9=77.8%	Li2S, SiP2, LiI	-0.335
	7/1	7/8=87.5%	Li2S, SiP, LiI	-0.322
1.31	0	0	P, Li2S, LiI	-0.339
	7/2	7/9=77.8%	Li2S, SiP2, LiI	-0.342
	7/1	7/8=87.5%	Li2S, SiP, LiI	-0.33
1.30	0	0	P, Li2S, LiI	-0.348
	7/2	7/9=77.8%	Li2S, SiP2, LiI	-0.35
	7/1	7/8=87.5%	Li2S, SiP, LiI	-0.337
1.29	0	0	P, Li2S, LiI	-0.357
	7/2	7/9=77.8%	Li2S, SiP2, LiI	-0.358
	7/1	7/8=87.5%	Li2S, SiP, LiI	-0.344
1.28	0	0	P, Li2S, LiI	-0.365
	7/2	7/9=77.8%	Li2S, SiP2, LiI	-0.366
	7/1	7/8=87.5%	Li2S, SiP, LiI	-0.352
1.27(→1.17)	0	0	LiP7, Li2S, LiI	-0.374
	7/2	7/9=77.8%	Li2S, SiP2, LiI	-0.374
	7/1	7/8=87.5%	Li2S, SiP, LiI	-0.359
1.26	0	0	LiP7, Li2S, LiI	-0.382
	7/2	7/9=77.8%	Li2S, SiP2, LiI	-0.382
	7/1	7/8=87.5%	Li2S, SiP, LiI	-0.366
1.25	0	0	LiP7, Li2S, LiI	-0.391
	7/2	7/9=77.8%	Li2S, SiP2, LiI	-0.39
	7/1	7/8=87.5%	Li2S, SiP, LiI	-0.373
1.24	0	0	LiP7, Li2S, LiI	-0.4
	7/2	7/9=77.8%	Li2S, SiP2, LiI	-0.397
	7/1	7/8=87.5%	Li2S, SiP, LiI	-0.381
1.23	0	0	LiP7, Li2S, LiI	-0.409
	7/2	7/9=77.8%	Li2S, SiP2, LiI	-0.405
	7/1	7/8=87.5%	Li2S, SiP, LiI	-0.388

1.22	0	0	LiP7, Li2S, LiI	-0.418
	7/2	7/9=77.8%	Li2S, SiP2, LiI	-0.413
	7/1	7/8=87.5%	Li2S, SiP, LiI	-0.395
1.21	0	0	LiP7, Li2S, LiI	-0.426
	7/2	7/9=77.8%	Li2S, SiP2, LiI	-0.421
	7/1	7/8=87.5%	Li2S, SiP, LiI	-0.403
1.20	0	0	LiP7, Li2S, LiI	-0.435
	7/2	7/9=77.8%	Li2S, SiP2, LiI	-0.429
	7/1	7/8=87.5%	Li2S, SiP, LiI	-0.41
1.19	0	0	LiP7, Li2S, LiI	-0.444
	7/2	7/9=77.8%	Li2S, SiP2, LiI	-0.437
	7/1	7/8=87.5%	Li2S, SiP, LiI	-0.417
1.18	0	0	LiP7, Li2S, LiI	-0.453
	7/2	7/9=77.8%	Li2S, SiP2, LiI	-0.445
	7/1	7/8=87.5%	Li2S, SiP, LiI	-0.424
1.17	0	0	LiP7, Li2S, LiI	-0.461
	7/2	7/9=77.8%	Li2S, SiP2, LiI	-0.453
	7/1	7/8=87.5%	Li2S, SiP, LiI	-0.432
1.16(→0.97)	0	0	Li3P7, Li2S, LiI	-0.47
	7/2	7/9=77.8%	Li2S, SiP2, LiI	-0.46
	7/1	7/8=87.5%	Li2S, SiP, LiI	-0.439
1.15	0	0	Li3P7, Li2S, LiI	-0.48
	7/2	7/9=77.8%	Li2S, SiP2, LiI	-0.468
	7/1	7/8=87.5%	Li2S, SiP, LiI	-0.446
1.14	0	0	Li3P7, Li2S, LiI	-0.489
	7/2	7/9=77.8%	Li2S, SiP2, LiI	-0.476
	7/1	7/8=87.5%	Li2S, SiP, LiI	-0.454
1.13	0	0	Li3P7, Li2S, LiI	-0.498
	7/2	7/9=77.8%	Li2S, SiP2, LiI	-0.484
	7/1	7/8=87.5%	Li2S, SiP, LiI	-0.461
1.12	0	0	Li3P7, Li2S, LiI	-0.507
	7/2	7/9=77.8%	Li2S, SiP2, LiI	-0.492
	7/1	7/8=87.5%	Li2S, SiP, LiI	-0.468
1.11	0	0	Li3P7, Li2S, LiI	-0.517
	7/2	7/9=77.8%	Li2S, SiP2, LiI	-0.5
	7/1	7/8=87.5%	Li2S, SiP, LiI	-0.476
1.10	0	0	Li3P7, Li2S, LiI	-0.526
	7/2	7/9=77.8%	Li2S, SiP2, LiI	-0.508
	7/1	7/8=87.5%	Li2S, SiP, LiI	-0.483
1.09	0	0	Li3P7, Li2S, LiI	-0.535
	7/2	7/9=77.8%	Li2S, SiP2, LiI	-0.515
	7/1	7/8=87.5%	Li2S, SiP, LiI	-0.49

1.08	0	0	Li3P7, Li2S, LiI	-0.544
	7/2	7/9=77.8%	Li2S, SiP2, LiI	-0.523
	7/1	7/8=87.5%	Li2S, SiP, LiI	-0.497
1.07	0	0	Li3P7, Li2S, LiI	-0.554
	7/2	7/9=77.8%	Li2S, SiP2, LiI	-0.531
	7/1	7/8=87.5%	Li2S, SiP, LiI	-0.505
1.06	0	0	Li3P7, Li2S, LiI	-0.563
	7/2	7/9=77.8%	Li2S, SiP2, LiI	-0.539
	7/1	7/8=87.5%	Li2S, SiP, LiI	-0.512
1.05	0	0	Li3P7, Li2S, LiI	-0.572
	7/2	7/9=77.8%	Li2S, SiP2, LiI	-0.547
	7/1	7/8=87.5%	Li2S, SiP, LiI	-0.519
1.04	0	0	Li3P7, Li2S, LiI	-0.582
	7/2	7/9=77.8%	Li2S, SiP2, LiI	-0.555
	7/1	7/8=87.5%	Li2S, SiP, LiI	-0.527
1.03	0	0	Li3P7, Li2S, LiI	-0.591
	7/2	7/9=77.8%	Li2S, SiP2, LiI	-0.563
	7/1	7/8=87.5%	Li2S, SiP, LiI	-0.534
1.02	0	0	Li3P7, Li2S, LiI	-0.6
	7/2	7/9=77.8%	Li2S, SiP2, LiI	-0.571
	7/1	7/8=87.5%	Li2S, SiP, LiI	-0.541
1.01	0	0	Li3P7, Li2S, LiI	-0.609
	7/2	7/9=77.8%	Li2S, SiP2, LiI	-0.578
	7/1	7/8=87.5%	Li2S, SiP, LiI	-0.548
1.00	0	0	Li3P7, Li2S, LiI	-0.619
	7/2	7/9=77.8%	Li2S, SiP2, LiI	-0.586
	7/1	7/8=87.5%	Li2S, SiP, LiI	-0.556
0.99	0	0	Li3P7, Li2S, LiI	-0.628
	7/2	7/9=77.8%	Li2S, SiP2, LiI	-0.594
	7/1	7/8=87.5%	Li2S, SiP, LiI	-0.563
0.98	0	0	Li3P7, Li2S, LiI	-0.637
	7/2	7/9=77.8%	Li2S, SiP2, LiI	-0.602
	7/1	7/8=87.5%	Li2S, SiP, LiI	-0.57
0.97	0	0	Li3P7, Li2S, LiI	-0.646
	7/2	7/9=77.8%	Li2S, SiP2, LiI	-0.61
	7/1	7/8=87.5%	Li2S, SiP, LiI	-0.578
0.96(→0.94)	0	0	Li3P7, Li2S, LiI	-0.656
	7/3	7/10=70%	Li2S, Li5SiP3, LiI	-0.632
	7/1	7/8=87.5%	Li2S, SiP, LiI	-0.585
0.95	0	0	Li3P7, Li2S, LiI	-0.665
	7/3	7/10=70%	Li2S, Li5SiP3, LiI	-0.643
	7/1	7/8=87.5%	Li2S, SiP, LiI	-0.592

0.94	0	0	Li3P7, Li2S, LiI	-0.674
	7/3	7/10=70%	Li2S, Li5SiP3, LiI	-0.653
	7/1	7/8=87.5%	Li2S, SiP, LiI	-0.599
0.93(→0.91)	0	0	LiP, Li2S, LiI	-0.684
	7/3	7/10=70%	Li2S, Li5SiP3, LiI	-0.664
	7/1	7/8=87.5%	Li2S, SiP, LiI	-0.607
0.92	0	0	LiP, Li2S, LiI	-0.694
	7/3	7/10=70%	Li2S, Li5SiP3, LiI	-0.675
	7/1	7/8=87.5%	Li2S, SiP, LiI	-0.614
0.91	0	0	LiP, Li2S, LiI	-0.704
	7/3	7/10=70%	Li2S, Li5SiP3, LiI	-0.686
	7/1	7/8=87.5%	Li2S, SiP, LiI	-0.621
0.90(→0.87)	0	0	LiP, Li2S, LiI	-0.714
	7/3	7/10=70%	Li2S, Li5SiP3, LiI	-0.697
0.89	0	0	LiP, Li2S, LiI	-0.725
	7/3	7/10=70%	Li2S, Li5SiP3, LiI	-0.707
0.88	0	0	LiP, Li2S, LiI	-0.735
	7/3	7/10=70%	Li2S, Li5SiP3, LiI	-0.718
0.87	0	0	LiP, Li2S, LiI	-0.745
	7/3	7/10=70%	Li2S, Li5SiP3, LiI	-0.729
0.86(→0.76)	0	0	Li3P, Li2S, LiI	-0.759
	7/3	7/10=70%	Li2S, Li5SiP3, LiI	-0.74
0.85	0	0	Li3P, Li2S, LiI	-0.772
	7/3	7/10=70%	Li2S, Li5SiP3, LiI	-0.75
0.84	0	0	Li3P, Li2S, LiI	-0.786
	7/3	7/10=70%	Li2S, Li5SiP3, LiI	-0.761
0.83	0	0	Li3P, Li2S, LiI	-0.8
	7/3	7/10=70%	Li2S, Li5SiP3, LiI	-0.772
0.82	0	0	Li3P, Li2S, LiI	-0.813
	7/3	7/10=70%	Li2S, Li5SiP3, LiI	-0.783
0.81	0	0	Li3P, Li2S, LiI	-0.827
	7/3	7/10=70%	Li2S, Li5SiP3, LiI	-0.793
0.80	0	0	Li3P, Li2S, LiI	-0.841
	7/3	7/10=70%	Li2S, Li5SiP3, LiI	-0.804
0.79	0	0	Li3P, Li2S, LiI	-0.854
	7/3	7/10=70%	Li2S, Li5SiP3, LiI	-0.815
0.78	0	0	Li3P, Li2S, LiI	-0.868
	7/3	7/10=70%	Li2S, Li5SiP3, LiI	-0.826
0.77	0	0	Li3P, Li2S, LiI	-0.882
	7/3	7/10=70%	Li2S, Li5SiP3, LiI	-0.837
0.76	0	0	Li3P, Li2S, LiI	-0.895
	7/3	7/10=70%	Li2S, Li5SiP3, LiI	-0.847

0.75(→0.40)	0	0	Li3P, Li2S, LiI	-0.909
0.74	0	0	Li3P, Li2S, LiI	-0.923
0.73	0	0	Li3P, Li2S, LiI	-0.936
0.72	0	0	Li3P, Li2S, LiI	-0.95
0.71	0	0	Li3P, Li2S, LiI	-0.964
0.7	0	0	Li3P, Li2S, LiI	-0.977
0.69	0	0	Li3P, Li2S, LiI	-0.991
0.68	0	0	Li3P, Li2S, LiI	-1.005
0.67	0	0	Li3P, Li2S, LiI	-1.018
0.66	0	0	Li3P, Li2S, LiI	-1.032
0.65	0	0	Li3P, Li2S, LiI	-1.046
0.64	0	0	Li3P, Li2S, LiI	-1.059
0.63	0	0	Li3P, Li2S, LiI	-1.073
0.62	0	0	Li3P, Li2S, LiI	-1.087
0.61	0	0	Li3P, Li2S, LiI	-1.1
0.6	0	0	Li3P, Li2S, LiI	-1.114
0.59	0	0	Li3P, Li2S, LiI	-1.128
0.58	0	0	Li3P, Li2S, LiI	-1.141
0.57	0	0	Li3P, Li2S, LiI	-1.155
0.56	0	0	Li3P, Li2S, LiI	-1.169
0.55	0	0	Li3P, Li2S, LiI	-1.182
0.54	0	0	Li3P, Li2S, LiI	-1.196
0.53	0	0	Li3P, Li2S, LiI	-1.209
0.52	0	0	Li3P, Li2S, LiI	-1.223
0.51	0	0	Li3P, Li2S, LiI	-1.237
0.5	0	0	Li3P, Li2S, LiI	-1.25
0.49	0	0	Li3P, Li2S, LiI	-1.264
0.48	0	0	Li3P, Li2S, LiI	-1.278
0.47	0	0	Li3P, Li2S, LiI	-1.291
0.46	0	0	Li3P, Li2S, LiI	-1.305
0.45	0	0	Li3P, Li2S, LiI	-1.319
0.44	0	0	Li3P, Li2S, LiI	-1.332
0.43	0	0	Li3P, Li2S, LiI	-1.346
0.42	0	0	Li3P, Li2S, LiI	-1.36
0.41	0	0	Li3P, Li2S, LiI	-1.373
0.4	0	0	Li3P, Li2S, LiI	-1.387
0.39	0	0	Li3P, Li2S, LiI	-1.401
		1	LiSi	-0.007
0.38(→0.37)	0	0	Li3P, Li2S, LiI	-1.414
		1	Li12Si7	-0.024
0.37	0	0	Li3P, Li2S, LiI	-1.428
		1	Li12Si7	-0.041

0.36(→0.18)	0	0	Li3P, Li2S, LiI	-1.442
		1	Li7Si3	-0.064
0.35	0	0	Li3P, Li2S, LiI	-1.455
		1	Li7Si3	-0.087
0.34	0	0	Li3P, Li2S, LiI	-1.469
		1	Li7Si3	-0.11
0.33	0	0	Li3P, Li2S, LiI	-1.483
		1	Li7Si3	-0.134
0.32	0	0	Li3P, Li2S, LiI	-1.496
		1	Li7Si3	-0.157
0.31	0	0	Li3P, Li2S, LiI	-1.51
		1	Li7Si3	-0.18
0.3	0	0	Li3P, Li2S, LiI	-1.524
		1	Li7Si3	-0.204
0.29	0	0	Li3P, Li2S, LiI	-1.537
		1	Li7Si3	-0.227
0.28	0	0	Li3P, Li2S, LiI	-1.551
		1	Li7Si3	-0.25
0.27	0	0	Li3P, Li2S, LiI	-1.565
		1	Li7Si3	-0.274
0.26	0	0	Li3P, Li2S, LiI	-1.578
		1	Li7Si3	-0.297
0.25	0	0	Li3P, Li2S, LiI	-1.592
		1	Li7Si3	-0.32
0.24	0	0	Li3P, Li2S, LiI	-1.606
		1	Li7Si3	-0.344
0.23	0	0	Li3P, Li2S, LiI	-1.619
		1	Li7Si3	-0.367
0.22	0	0	Li3P, Li2S, LiI	-1.633
		1	Li7Si3	-0.39
0.21	0	0	Li3P, Li2S, LiI	-1.647
		1	Li7Si3	-0.414
0.2	0	0	Li3P, Li2S, LiI	-1.66
		1	Li7Si3	-0.437
0.19	0	0	Li3P, Li2S, LiI	-1.674
		1	Li7Si3	-0.46
0.18	0	0	Li3P, Li2S, LiI	-1.688
		1	Li7Si3	-0.484
0.17(→0.13)	0	0	Li3P, Li2S, LiI	-1.701
		1	Li13Si4	-0.515
0.16	0	0	Li3P, Li2S, LiI	-1.715
		1	Li13Si4	-0.548

0.15	0	0	Li3P, Li2S, LiI	-1.729
		1	Li13Si4	-0.58
0.14	0	0	Li3P, Li2S, LiI	-1.742
		1	Li13Si4	-0.613
0.13	0	0	Li3P, Li2S, LiI	-1.756
		1	Li13Si4	-0.645
0.12(→0)	0	0	Li3P, Li2S, LiI	-1.769
		1	Li21Si5 (dashed)	-0.679
0.11	0	0	Li3P, Li2S, LiI	-1.783
		1	Li21Si5 (dashed)	-0.721
0.1	0	0	Li3P, Li2S, LiI	-1.797
		1	Li21Si5 (dashed)	-0.763
0.09	0	0	Li3P, Li2S, LiI	-1.81
		1	Li21Si5 (dashed)	-0.805
0.08	0	0	Li3P, Li2S, LiI	-1.824
		1	Li21Si5 (dashed)	-0.847
0.07	0	0	Li3P, Li2S, LiI	-1.838
		1	Li21Si5 (dashed)	-0.889
0.06	0	0	Li3P, Li2S, LiI	-1.851
		1	Li21Si5 (dashed)	-0.931
0.05	0	0	Li3P, Li2S, LiI	-1.865
		1	Li21Si5 (dashed)	-0.973
0.04	0	0	Li3P, Li2S, LiI	-1.879
		1	Li21Si5 (dashed)	-1.015
0.03	0	0	Li3P, Li2S, LiI	-1.892
		1	Li21Si5 (dashed)	-1.057
0.02	0	0	Li3P, Li2S, LiI	-1.906
		1	Li21Si5 (dashed)	-1.099
0.01	0	0	Li3P, Li2S, LiI	-1.92
		1	Li21Si5 (dashed)	-1.141
0	0	0	Li3P, Li2S, LiI	-1.933
		1	Li21Si5 (dashed)	-1.183

Table S3. Summary of calculated electrochemical stability between Si and LBHI

Voltage (V vs. Li/Li+)	Ratio, Si/LBHI	Molar ratio, Si/(Si+LBHI)	Reaction products	**E**rxtrxt (eV/atom)
1.50(→0.53)	0	0	(none)	(none)
0.52(→0.40)	0	0	LiH, Li(BH)6, LiI	-0.004
0.51	0	0	LiH, Li(BH)6, LiI	-0.008
0.5	0	0	LiH, Li(BH)6, LiI	-0.012
0.49	0	0	LiH, Li(BH)6, LiI	-0.016
0.48	0	0	LiH, Li(BH)6, LiI	-0.02
0.47	0	0	LiH, Li(BH)6, LiI	-0.024
0.46	0	0	LiH, Li(BH)6, LiI	-0.028
0.45	0	0	LiH, Li(BH)6, LiI	-0.032
0.44	0	0	LiH, Li(BH)6, LiI	-0.036
0.43	0	0	LiH, Li(BH)6, LiI	-0.04
0.42	0	0	LiH, Li(BH)6, LiI	-0.044
0.41	0	0	LiH, Li(BH)6, LiI	-0.048
0.4	0	0	LiH, Li(BH)6, LiI	-0.052
0.39	0	0	LiH, Li(BH)6, LiI	-0.056
		1	LiSi	-0.007
0.38	0	0	LiH, Li(BH)6, LiI	-0.061
	1/2	1/3	LiH, LiSiB6, LiI	-0.06
		1	Li12Si7	-0.024
0.37	0	0	LiH, LiB3, LiI	-0.065
	1/2	1/3	LiH, LiSiB6, LiI	-0.066
		1	Li12Si7	-0.041
0.36	0	0	LiH, LiB3, LiI	-0.071
	1/2	1/3	LiH, LiSiB6, LiI	-0.071
		1	Li7Si3	-0.064
0.35(→0.18)	0	0	LiH, LiB3, LiI	-0.077
		1	Li7Si3	-0.087
0.34	0	0	LiH, LiB3, LiI	-0.084
		1	Li7Si3	-0.110
0.33	0	0	LiH, LiB3, LiI	-0.09
		1	Li7Si3	-0.134
0.32	0	0	LiH, LiB3, LiI	-0.096
		1	Li7Si3	-0.157
0.31	0	0	LiH, LiB3, LiI	-0.102
		1	Li7Si3	-0.18
0.3	0	0	LiH, LiB3, LiI	-0.109
		1	Li7Si3	-0.204
0.29	0	0	LiH, LiB3, LiI	-0.115
		1	Li7Si3	-0.227

0.28	0	0	LiH, LiB3, LiI	-0.121
		1	Li7Si3	-0.25
0.27	0	0	LiH, LiB3, LiI	-0.127
		1	Li7Si3	-0.274
0.26	0	0	LiH, LiB3, LiI	-0.134
		1	Li7Si3	-0.297
0.25	0	0	LiH, LiB3, LiI	-0.14
		1	Li7Si3	-0.32
0.24	0	0	LiH, LiB3, LiI	-0.146
		1	Li7Si3	-0.344
0.23	0	0	LiH, LiB3, LiI	-0.152
		1	Li7Si3	-0.367
0.22	0	0	LiH, LiB3, LiI	-0.159
		1	Li7Si3	-0.39
0.21	0	0	LiH, LiB3, LiI	-0.165
		1	Li7Si3	-0.414
0.20	0	0	LiH, LiB3, LiI	-0.171
		1	Li7Si3	-0.437
0.19	0	0	LiH, LiB3, LiI	-0.177
		1	Li7Si3	-0.46
0.18	0	0	LiH, LiB3, LiI	-0.184
		1	Li7Si3	-0.484
0.17(→0.13)	0	0	LiH, LiB3, LiI	-0.19
		1	Li13Si4	-0.515
0.16	0	0	LiH, LiB3, LiI	-0.196
		1	Li13Si4	-0.548
0.15	0	0	LiH, LiB3, LiI	-0.202
		1	Li13Si4	-0.58
0.14	0	0	LiH, LiB3, LiI	-0.209
		1	Li13Si4	-0.613
0.13	0	0	LiH, LiB3, LiI	-0.215
		1	Li13Si4	-0.645
0.12(→0.05)	0	0	LiH, LiB3, LiI	-0.221
		1	Li21Si5 (dashed)	-0.679
0.11	0	0	LiH, LiB3, LiI	-0.227
		1	Li21Si5 (dashed)	-0.721
0.10	0	0	LiH, LiB3, LiI	-0.234
		1	Li21Si5 (dashed)	-0.763
0.09	0	0	LiH, LiB3, LiI	-0.24
		1	Li21Si5 (dashed)	-0.805
0.08	0	0	LiH, LiB3, LiI	-0.246
		1	Li21Si5 (dashed)	-0.847

0.07	0	0	LiH, LiB3, LiI	-0.252
		1	Li21Si5 (dashed)	-0.889
0.06	0	0	LiH, LiB3, LiI	-0.259
		1	Li21Si5 (dashed)	-0.931
0.05	0	0	LiH, LiB3, LiI	-0.265
		1	Li21Si5 (dashed)	-0.973
0.04(→0)	0	0	LiH, LiB, LiI	-0.271
		1	Li21Si5 (dashed)	-1.015
0.03	0	0	LiH, LiB, LiI	-0.279
		1	Li21Si5 (dashed)	-1.057
0.02	0	0	LiH, LiB, LiI	-0.286
		1	Li21Si5 (dashed)	-1.099
0.01	0	0	LiH, LiB, LiI	-0.294
		1	Li21Si5 (dashed)	-1.141
0	0	0	LiH, LiB, LiI	-0.301
		1	Li21Si5 (dashed)	-1.183

Table S4.1 Summary of calculated chemical stability between Si and LBHI

Molar ratio, Si/(Si+LBH4-LI)	Reaction products	**E**rxtrxt (eV/atom)
0	LBHI	0
1	Si	0

Table S4.2 Summary of calculated chemical stability between Si and LPSI

Molar ratio, Si/(Si+LPS-LI)	Reaction products	**E**rxtrxt (eV/atom)
0	LPSI	0
0.7778	Li10Si(PS6)2, LiI, SiS2, P	-0.047
0.8974	Li2S, LiI, SiS2, P	-0.096
0.9245	SiP2, Li2S, LiI, SiS2	-0.108
0.9403	SiP, Li2S, LiI, SiS2	-0.111
1	Si	0

Table S4.3 Summary of calculated chemical stability between Si and LPS

Molar ratio, Si/(Si+LPS)	Reaction products	**E**rxtrxt (eV/atom)
0	LPS	0
0.3333	Li10Si(PS6)2, LiI, SiS2, P	-0.056
0.5555	Li2S, SiS2, P	-0.114
0.6364	SiP2, Li2S, SiS2	-0.128
0.6923	SiP, Li2S, SiS2	-0.129
1	Si	0

Table S5.1 Summary of calculated chemical stability between Li15Si4 and LBHI

Molar ratio, Li15Si4/(Li15Si4+LBHI)	Reaction products	**E**rxtrxt (eV/atom)
0	LBHI	0
0.3023	Li(BH)6, LiH, LiI, Si	-0.053
0.3714	LiSi, Li(BH)6, LiH, LiI	-0.056
0.4439	Li12Si7, Li(BH)6, LiH, LiI	-0.058
0.5149	Li12Si7, LiSiB6, LiH, LiI	-0.059
0.5952	LiSiB6, Li7Si3, LiH, LiI	-0.06
0.7975	Li13Si4, LiSiB6, LiH, LiI	-0.035
1	Li13Si4, Li21Si5	-0.003

Table S5.2 Summary of calculated chemical stability between Li15Si4 and LPSI

Molar ratio, Li15Si4/(Li15Si4+LPSI)	Reaction products	**E**rxtrxt (eV/atom)
0	LPSI	0
0.3302	Li10Si(PS6)2, Li2S, LiI, P	-0.161
0.5303	Li2S, LiI, SiS2, P	-0.31
0.6125	SiP2, Li2S, LiI, SiS2	-0.379
0.6702	SiP, Li2S, LiI, SiS2	-0.43
0.7	SiP, Li2S, LiI, Si	-0.456
0.7568	Li5SiP3, Li2S, LiI, Si	-0.459
0.7887	Li3P, Li2S, LiI, Si	-0.451
0.8358	LiSi, Li3P, Li2S, LiI	-0.392
0.8731	Li12Si7, Li3P, Li2S, LiI	-0.338
0.9081	Li7Si3, Li3P, Li2S, LiI	-0.277
0.9655	Li13Si4, Li3P, Li2S, LiI	-0.123
1	Li13Si4, Li21Si5	-0.003

Table S5.3 Summary of calculated chemical stability between Li15Si4 and LPS

Molar ratio, Li15Si4/(Li15Si4+LPS)	Reaction products	**E**rxtrxt (eV/atom)
0	LPS	0
0.0658	Li10Si(PS6)2, Li2S, P	-0.191
0.1389	SiS2, Li2S, P	-0.358
0.1842	SiP2, SiS2, Li2S	-0.432
0.225	SiP, SiS2, Li2S	-0.485
0.25	SiP, Li2S, Si	-0.511
0.3077	Li5SiP3, Li2S, Si	-0.506
0.3478	Li3P, Li2S, Si	-0.493
0.4211	LiSi, Li3P, Li2S	-0.423
0.4956	Li12Si7, Li3P, Li2S	-0.36
0.5854	Li7Si3, Li3P, Li2S	-0.291
0.8	Li13Si4, Li3P, Li2S	-0.126
1	Li13Si4, Li21Si5	-0.003

Table S6. References for ICEs

References	ICE/%	Paper title
L1	59.9	Disposing of excessive decomposition and destructive intercalation of solvated Li+ in CNT-based flexible 3D Si anode of flexible battery
L2	70	Rationally engineered amorphous TiOx/Si/TiOx nanomembrane as an anode material for high energy lithium ion battery
L3	74	Silicene Flowers: A Dual Stabilized Silicon Building Block for High-Performance Lithium Battery Anodes
L4	75.32	Overcome the fundamental challenge for PVDF binder to use with silicon anode with super-molecular nano-layer
L5	78.5	Hollow Si nanospheres with amorphous TiO2 layer used as anode for high-performance Li-ion battery
L6	79.1	Synthesis of Ultrathin Silicon Nanosheets by Using Graphene Oxide as Template
L7	80	Water-Soluble Polymer Assists Multisize Three-Dimensional Microspheres as a High-Performance Si Anode for Lithium-Ion Batteries
L8	80.1	Mesoporous Silicon Hollow Nanocubes Derived from Metal–Organic Framework Template for Advanced Lithium-Ion Battery Anode
	80.1	Sustainable silicon micro-dendritic anodes integrated by a moderately cross-linked polymer binder with superior elasticity and adhesion
L9	81	Vapor-solid-solid growth of silicon nanowires using magnesium seeds and their electrochemical performance in Li-ion battery anodes
L10	81.2	Si nanoparticles confined within a conductive 2D porous Cu-based metal–organic framework (Cu3(HITP)2) as potential anodes for high-capacity Li-ion batteries
	81.2	Self-standing mesoporous Si films as anodes for lithium-ion microbatteries
L11	81.4	Reversible Storage of Lithium in Silver-Coated Three-Dimensional Macroporous Silicon
L12	82.5	Synthesis of 3D stacked silicon nanosheets via electrochemical reduction of attapulgite in molten salt for high-performance lithium-ion batteries anode
L13	83	Confining invasion directions of Li+ to achieve efficient Si anode material for lithium-ion batteries
L14	83.1	Self-Templating Construction of 3D Hierarchical Macro-Mesoporous Silicon from 0D Silica Nanoparticles
L15	83.6	In-situ migration of Ni induced crystallization to boost the initial coulombic efficiency of nano Si anode for lithium ion batteries

L16	84	High-performance lithium-ion battery with nano-porous polycrystalline silicon particles as anode
L17	85	Bulk-Nanoporous-Silicon Negative Electrode with Extremely High Cyclability for Lithium-Ion Batteries Prepared Using a Top-Down Process
L18	86	High-capacity silicon electrodes obtained from the hydrogen production process by aluminum alloy hydrolysis
	86	Effect of vinylene carbonate electrolyte additive and battery cycling protocol on the electrochemical and cyclability performance of silicon thin-film anodes
L19	86.4	Ionically Conductive Self-Healing Polymer Binders with Poly(ether-thioureas) Segments for High-Performance Silicon Anodes in Lithium-Ion Batteries
L20	86.5	Effect of Size and Shape on Electrochemical Performance of Nano-Silicon-Based Lithium Battery
L21	86.7	Dual Cross-Linked Polymer Networks Derived from the Hyperbranched Poly(ethyleneimine) and Poly(acrylic acid) as Efficient Binders for Silicon Anodes in Lithium-Ion Batteries
L22	87.9	Surface-Oxidation-Induced Constrained Volume Expansion of Commercial Silicon Flakes as High-Performance Anode Material for Lithium-Ion Batteries
L23	88	Nanoporous silicon prepared through air-oxidation demagnesiation of Mg2Si and properties of its lithium ion batteries
L24	88.1	High-yield synthesis of ultrathin silicon nanosheets by physical grinding enables robust lithium-ion storage
L25	89	Si nanoflake-assembled blocks towards high initial coulombic efficiency anodes for lithium-ion batteries
	89	Boron-doped porous Si anode materials with high initial coulombic efficiency and long cycling stability
L26	89.5	Novel constructive self-healing binder for silicon anodes with high mass loading in lithium-ion batteries
L27	89.6	Effects of Pyrolysis on High-Capacity Si-Based Anode of Lithium Ion Battery with High Coulombic Efficiency and Long Cycling Life
L28	90.2	Electrolyte Design Enabling a High-Safety and High- Performance Si Anode with a Tailored Electrode–Electrolyte Interphase
L29	90.4	A compared investigation of different biogum polymer binders for silicon anode of lithium-ion batteries
L30	91	Carboxymethylated tamarind polysaccharide gum as a green binder for silicon-based lithium-ion battery anodes
L31	91.1	In Situ Polymerized and Imidized Si@Polyimide Microcapsules with Flexible Solid-Electrolyte Interphase and Enhanced Electrochemical Activity for Li-Storage

L32	91.4	Regulating adhesion of solid-electrolyte interphase to silicon via covalent bonding strategy towards high Coulombic-efficiency anodes
L33	92	A Highly Efficient Silicone-Modified Polyamide Acid Binder for Silicon-Based Anode in Lithium-Ion Batteries
	92	Improving Electrochemical Performance of Thick Silicon Film Anodes with Implanted Solid Lithium Source Electrolyte
L34	92.7	Multiscale Hyperporous Silicon Flake Anodes for High Initial Coulombic Efficiency and Cycle Stability
L35	93.2	Silicon Anode with High Initial Coulombic Efficiency by Modulated Trifunctional Binder for High-Areal-Capacity Lithium-Ion Batteries
	93.2	Cross-Linking Network of Soft–Rigid Dual Chains to Effectively Suppress Volume Change of Silicon Anode
S1	54	Electrochemical Performance of All-Solid-State Li-Ion Batteries Based on Garnet Electrolyte Using Silicon as a Model Electrode
S2	60.1	Sustainable Interfaces between Si Anodes and Garnet Electrolytes for Room-Temperature Solid-State Batteries
S3	64.5	Si nanoparticles embedded in carbon nanofiber sheathed with Li6PS5Cl as an anode material for all-solid-state batteries
S4	69	Microscopic observation of nanoporous Si-Li3PS4 interface in composite anodes with stable cyclability
	69	Performance improvement of nanoporous Si composite anodes in all-solid-state lithium-ion batteries by using acetylene black as a conductive additive
S5	71	Stable cyclability of porous Si anode applied for sulfide-based all-solid-state batteries
	71	Stable Cyclability Caused by Highly Dispersed Nanoporous Si Composite Anodes with Sulfide-based Solid Electrolyte
S6	83.2	A silicon anode for garnet-based all-solid-state batteries/ Interfaces and nanomechanics
S7	84	Enabling High-Energy Solid-State Batteries with Stable Anode Interphase by the Use of Columnar Silicon Anodes
S8	85.6	Microstructure Study of Electrochemically Driven LixSi
	85.6	Long-Cycling Sulfide-Based All-Solid-State Batteries Enabled by Electrochemo-Mechanically Stable Electrodes
S9	92	An amorphous Si film anode for all-solid-state lithium batteries
S10	94	Porous amorphous silicon film anodes for high- capacity and stable all-solid-state lithium batteries

Table S7. Theoretical volume change of Si-LPS composite after lithiation from 1.5 to 0 V vs. Li$^+$/Li. The reactions are obtained from Table S1. Here, the bulk volume (V, normalized by formula unit) of each chemical, the total volume (V_{tot}) of precursors and products, as well as the ratio (V_{tot} ratio) of product volume over precursor volume are listed for each reaction.

0–0.12 V	Precursors		→	Products
	Si	4.2Li	→	0.2Li21Si5
V (A^3/formula unit)	20.44375	20.11		397.815625
V_{tot} (A^3)	20.44375 (without Li)			79.563125
V_{tot} ratio	389.18%			

0.13–0.17 V	Precursors		→	Products
	Si	3.25Li	→	0.25Li13Si4
V (A^3/formula unit)	20.44375	20.11		262.065
V_{tot} (A^3)	20.44375 (without Li)			65.51625
V_{tot} ratio	320.47%			

0.18–0.36 V	Precursors		→	Products
	Si	2.333Li	→	0.3333Li7Si3
V (A^3/formula unit)	20.44375	20.11		149.293333
V_{tot} (A^3)	20.44375 (without Li)			49.76444
V_{tot} ratio	243.42%			

0.37–0.38 V	Precursors		→	Products
	Si	1.714Li	→	0.1429Li12Si7
V (A^3/formula unit)	20.44375	20.11		299.5025
V_{tot} (A^3)	20.44375 (without Li)			42.7989
V_{tot} ratio	209.35%			

0.39 V	Precursors		→	Products
	Si	Li	→	LiSi
V (A^3/formula unit)	20.44375	20.11		31.21375
V_{tot} (A^3)	20.44375 (without Li)			31.21375
V_{tot} ratio	152.68%			

0–0.86 V	Precursors		→	Products	
	4Li3PS4	32Li	→	4Li3P	16Li2S
V (A^3/formula unit)	166.5375	20.11		58.82	46.82
V_{tot} (A^3)	666.15 (without Li)			984.4	
V_{tot} ratio	147.77%				

0.76–0.96 V	Precursors			→	Products	
	1.714Li3PS4	0.5714Si	11.43Li	→	0.5714Li5SiP3	6.857Li2S
V (A^3/formula unit)	166.5375	20.44375	20.11		154	46.82
V_{tot} (A^3)	297.1268338 (without Li)				409.04034	
V_{tot} ratio	137.67%					

0.87–0.93 V	Precursors		→	Products	
	4Li3PS4	24Li	→	4LiP	16Li2S
V (A^3/formula unit)	166.5375	20.11		31.41	46.82
V_{tot} (A^3)	666.15 (without Li)			874.76	
V_{tot} ratio	131.32%				

0.91–1.49 V	Precursors			→	Products	
	0.8Li3PS4	0.8Si	4Li	→	0.8SiP	3.2Li2S
V (A^3/formula unit)	166.5375	20.44375	20.11		47.233	46.82
V_{tot} (A^3)	149.585 (without Li)				187.6104	
V_{tot} ratio	125.42%					

0.94–1.16 V	Precursors		→	Products	
	4Li3PS4	21.71Li	→	0.5714Li3P7	16Li2S
V (A^3/formula unit)	166.5375	20.11		199.0325	46.82
V_{tot} (A^3)	666.15 (without Li)			862.8471705	
V_{tot} ratio	129.53%				

0.97–1.49 V	Precursors			→	Products	
	1.333Li3PS4	0.6667Si	6.667Li	→	0.6667SiP2	5.333Li2S
V (A^3/formula unit)	166.5375	20.44375	20.11		70.8325	46.82
V_{tot} (A^3)	235.6243356 (without Li)				296.9150878	
V_{tot} ratio	126.01%					

1.17–1.27 V	Precursors		→	Products	
	4Li3PS4	20.57Li	→	0.5714LiP7	16Li2S
V (A^3/formula unit)	166.5375	20.11		117.64	46.82
V_{tot} (A^3)	666.15 (without Li)			816.339496	
V_{tot} ratio	122.55%				

1.28–1.49 V	Precursors		→	Products	
	4Li3PS4	20Li	→	4P	16Li2S
V (A^3/formula unit)	166.5375	20.11		26.52166	46.82
V_{tot} (A^3)	666.15 (without Li)			855.20664	
V_{tot} ratio	128.38%				

Table S8. Theoretical volume change of Si-LPSI composite after lithiation from 1.5 to 0 V vs. Li^+/Li. The reactions are obtained from Table S2. Here, the bulk volume (V, normalized by formula unit) of each chemical, the total volume (V_{tot}) of precursors and products, as well as the ratio (V_{tot} ratio) of product volume over precursor volume are listed for each reaction.

0–0.12 V	Precursors		→	Products
	Si	4.2Li	→	0.2Li21Si5
V (A^3/formula unit)	20.44375	20.11		397.815625
V_{tot} (A^3)	20.44375 (without Li)			79.563125
V_{tot} ratio	389.18%			

0.13–0.17 V	Precursors		→	Products
	Si	3.25Li	→	0.25Li13Si4
V (A^3/formula unit)	20.44375	20.11		262.065
V_{tot} (A^3)	20.44375 (without Li)			65.51625
V_{tot} ratio	320.47%			

0.18–0.36 V	Precursors		→	Products
	Si	2.333Li	→	0.3333Li7Si3
V (A^3/formula unit)	20.44375	20.11		149.293333
V_{tot} (A^3)	20.44375 (without Li)			49.76444
V_{tot} ratio	243.42%			

0.37–0.38 V	Precursors		→	Products
	Si	1.714Li	→	0.1429Li12Si7
V (A^3/formula unit)	20.44375	20.11		299.5025
V_{tot} (A^3)	20.44375 (without Li)			42.7989
V_{tot} ratio	209.35%			

0.39 V	Precursors		→	Products
	Si	Li	→	LiSi
V (A^3/formula unit)	20.44375	20.11		31.21375
V_{tot} (A^3)	20.44375 (without Li)			31.21375
V_{tot} ratio	152.68%			

0–0.86 V	Precursors		→	Products		
	Li27P7(S14I3)2	56Li	→	7Li3P	28Li2S	6LiI
V (A^3/formula unit)	1567.8825	20.11		58.82	46.82	67.02
V$_{tot}$ (A^3)	1567.8825 (without Li)			2124.82		
V$_{tot}$ ratio	135.52%					

0.76–0.96 V	Precursors			→	Products		
	0.3Li27P7(S14I3)2	0.7Si	14Li	→	0.7Li5SiP3	8.4Li2S	1.8LiI
V (A^3/formula unit)	1567.8825	20.44375	20.11		154	46.82	67.02
V$_{tot}$ (A^3)	484.675375 (without Li)				621.724		
V$_{tot}$ ratio	128.28%						

0.87–0.93 V	Precursors		→	Products		
	Li27P7(S14I3)2	42Li	→	7LiP	28Li2S	6LiI
V (A^3/formula unit)	1567.8825	20.11		31.41	46.82	67.02
V$_{tot}$ (A^3)	1567.8825 (without Li)			1932.95		
V$_{tot}$ ratio	123.28%					

0.91–1.49 V	Precursors			→	Products		
	0.125 Li27P7(S14I3)2	0.875Si	4.375Li	→	0.875SiP	3.5Li2S	0.75LiI
V (A^3/formula unit)	1567.8825	20.44375	20.11		47.233	46.82	67.02
V$_{tot}$ (A^3)	213.8735938 (without Li)				255.463875		
V$_{tot}$ ratio	119.45%						

0.94–1.16 V	Precursors		→	Products		
	Li27P7(S14I3)2	38Li	→	Li3P7	28Li2S	6LiI
V (A^3/formula unit)	1567.8825	20.11		199.0325	46.82	67.02
V$_{tot}$ (A^3)	1567.8825 (without Li)			1912.1125		
V$_{tot}$ ratio	121.96%					

0.97–1.49 V	Precursors			→	Products		
	0.2222Li27P7(S14I3)2	0.7778Si	7.778Li	→	0.7778SiP2	6.222Li2S	1.333LiI
V (A^3/formula unit)	1567.8825	20.44375	20.11		70.8325	46.82	67.02
V$_{tot}$ (A^3)	364.2846403 (without Li)				435.7452185		
V$_{tot}$ ratio	119.62%						

1.17–1.27 V	Precursors		→	Products		
	Li27P7(S14I3)2	36Li	→	LiP7	28Li2S	6LiI
V (A^3/formula unit)	1567.8825	20.11		117.64	46.82	67.02
V$_{tot}$ (A^3)	1567.8825 (without Li)			1830.72		
V$_{tot}$ ratio	116.76%					

1.28–1.49 V	Precursors		→	Products		
	Li27P7(S14I3)2	35Li	→	7P	28Li2S	6LiI
V (A^3/formula unit)	1567.8825	20.11		26.52166	46.82	67.02
V$_{tot}$ (A^3)	1567.8825 (without Li)			1898.73162		
V$_{tot}$ ratio	121.10%					

Table S9. Theoretical volume change of Si-LBHI composite after lithiation from 1.5 to 0 V vs. Li^+/Li. The reactions are obtained from Table S3. Here, the bulk volume (V, normalized by formula unit) of each chemical, the total volume (V_{tot}) of precursors and products, as well as the ratio (V_{tot} ratio) of product volume over precursor volume are listed for each reaction.

0–0.12 V	Precursors		→	Products
	Si	4.2Li	→	0.2Li21Si5
V (A^3/formula unit)	20.44375	20.11		397.815625
V_{tot} (A^3)	20.44375 (without Li)			79.563125
V_{tot} ratio	389.18%			

0.13–0.17 V	Precursors		→	Products
	Si	3.25Li	→	0.25Li13Si4
V (A^3/formula unit)	20.44375	20.11		262.065
V_{tot} (A^3)	20.44375 (without Li)			65.51625
V_{tot} ratio	320.47%			

0.18–0.36 V	Precursors		→	Products
	Si	2.333Li	→	0.3333Li7Si3
V (A^3/formula unit)	20.44375	20.11		149.293333
V_{tot} (A^3)	20.44375 (without Li)			49.76444
V_{tot} ratio	243.42%			

0.37–0.38 V	Precursors		→	Products
	Si	1.714Li	→	0.1429Li12Si7
V (A^3/formula unit)	20.44375	20.11		299.5025
V_{tot} (A^3)	20.44375 (without Li)			42.7989
V_{tot} ratio	209.35%			

0.39 V	Precursors		→	Products
	Si	Li	→	LiSi
V (A^3/formula unit)	20.44375	20.11		31.21375
V_{tot} (A^3)	20.44375 (without Li)			31.21375
V_{tot} ratio	152.68%			

0–0.04 V	Precursors		→	Products		
	Li4B3H12I	12Li	→	12LiH	3LiB	LiI
V (A^3/formula unit)	233.0325	20.11		16.0025	21.725	67.02
V_{tot} (A^3)	233.0325 (without Li)			324.225		
V_{tot} ratio	139.13%					

0.05–0.37 V	Precursors		→	Products		
	Li4B3H12I	10Li	→	12LiH	LiB3	LiI
V (A^3/formula unit)	233.0325	20.11		16.0025	37.23	67.02
V_{tot} (A^3)	233.0325 (without Li)			296.28		
V_{tot} ratio	127.14%					

0.36–0.38 V	Precursors			→	Products		
	0.6667Li4B3H12I	0.3333Si	6.333Li	→	0.3333LiSiB6	8LiH	0.6667LiI
V (A^3/formula unit)	233.0325	20.44375	20.11		70.85875	16.0025	67.02
V_{tot} (A^3)	162.1766696 (without Li)				196.3194554		
V_{tot} ratio	121.05 %						

0.38–0.52 V	Precursors		→	Products		
	Li4B3H12I	6.5Li	→	9LiH	0.5Li(BH)6	LiI
V (A^3/formula unit)	233.0325	20.11		16.0025	111.96875	67.02
V_{tot} (A^3)	233.0325 (without Li)			267.026875		
V_{tot} ratio	114.59 %					